DENDRITIC POLYMERS AS BIOCOMPATIBLE OIL SPILL DISPERSANTS: EFFECTIVENESS AND MECHANISIMS WITH CRUDE OIL

A Thesis
Presented to
the Graduate School of
Clemson University

In Partial Fulfillment
of the Requirements for the Degree
Master of Science
Environmental Engineering and Earth Sciences

---

by
Ying Tu
August 2014

Accepted by:
Dr. David Ladner, Committee Chair
Dr. Tanju Karanfil
Dr. David Freedman

ABSTRACT

Dendritic polymers have recently been shown to entrap polycyclic aromatic hydrocarbons (PAHs) and other hydrophobic materials. Laboratory results have shown that poly(amidoamine) dendrimers and hyperbranched poly(ethyleneimine) polymers form complexes with linear (hexadecane) and polyaromatic (phenanthrene) hydrocarbons, increasing the dispersion of these model crude oil components. It is thus hypothesized that crude oil can be dispersed using these polymers. Compared with commercial dispersants, dendritic polymers have the potential to be more biocompatible and less toxic.

The objective of this research was to gain a fundamental understanding of the interactions of dendritic polymers with crude oil. We used Louisians Sweet Crude oil to explore the dispersion effectiveness of the polymers and the mechanisms of oil-polymer interactions. Results were compared with Corexit 9500, the dispersant used in response to the Deepwater Horizon disaster of 2010. We investigated the factors that may influence the experimental results, such as dispersant to oil ratio (DOR), mixing and settling time, sample preparation methods and sample collection methods to establish experimental protocols that adequately characterized the effectiveness of the polymers.

The effects of polymer size and surface groups on oil dispersion effectiveness were examined through an optimized effectiveness test. Five hyperbranched polyethylenimine polymers (HY-PEI) with molecular weight 1.2, 1.8, 10, 70 and 750 kDa and amino surface terminal groups were examined with the effectiveness test. The results

showed the 10 kDa HY-PEI had the highest dispersion efficiency (58%) slightly larger than Corexit (56%). 70 kDa and 750 kDa HY-PEI also had a relatively high effectiveness, 48% and 40% respectively; however, the low molecular weight polymers, 1.2 kDa and 1.8 kDa had low dispersion efficiency, 11% and 17%, similar to the no dispersant scenario which had 13% oil dispersion.

We also tested three dendrimers with different surface terminal groups: amino (positive charge), amidoethanol (neutral charge) and succinamic acid (negative charge). The results showed that G4-PAMAM-NH_2 with positive surface charge had the highest efficiency of these three, 42%. G4-PAMAM-OH and G4-PAMAM-SA had lower dispersion capacity, with effectiveness of 16% and 19%.

We concluded that the polymers with moderate size and positive charged surface groups are very capable in dispersing light sweet crude oil. Further exploring the interactions of dendritic polymers with crude oil, we conducted dynamic interfacial tension test and oil droplet size distribution test. The dynamic interfacial tension curves shows that all the polymers can reduce the interfacial tension and the larger polymers are more capable at decreasing the interfacial tension rapidly. The efficiency of polymer dispersion for oil has also been verified by drop size distribution measurements. Polymers with high performance in effectiveness test tend to create smaller droplets than polymers that show less effectiveness. Again, moderately sized polymers gave the smaller average droplet size and polydispersity. By further analyzing the data we developed a conceptual model for the oil dendritic polymer interaction, which is a hybrid surfactant and Pickering emulsion mechanism.

DEDICATION

I would like to dedicate my thesis to my family, who has always been supportive of my endeavors.

ACKNOWLEDGEMENTS

I would like to acknowledge my advisor, Dr. David Ladner, who was willing to meet with me on a weekly basis to discuss my results and future experiments. I would also like to acknowledge Dr. Tanju Karanfil and Dr. David Freedman for their willingness to be members of my committee.

I would like to acknowledge my coworkers Nicholas K. Geitner, Pu-Chun Ke, and Feng Ding who provided lots of useful experimental results and instructive opinions. I would like to acknowledge Peng Xie, Muriel Steele, Mengfei Li, Jiankun Cai and Erin Partlan for their help with the experiments. Also, I am thankful to Cassie Gregory for sharing the cell counter with me. I would like to thank Rhonda Powell for helping me with my imaging.

TABLE OF CONTENTS

Page

TABLE OF CONTENTS (CONTINUED)

Page

TABLE OF CONTENTS (CONTINUED)

Page

LIST OF TABLES

Page

LIST OF FIGURES

Page

LIST OF FIGURES (CONTINUED)

Page

LIST OF SYMBOLS AND ABBREVIATIONS

Abbreviations

ADSA	Axisymmetric Drop Shape Analysis
APD	Avalanche Photodiode Detector
CB	Carbon Black
DCM	Dichloromethane
DLVO	Derjaguin, Landau, Verwey, and Overbeek
DOR	Dispersant to Oil Ratio
DSA	Drop Shape Analysis
G4	Generation 4th
HLB	Hydrophlic Lipophile Balance
HMC	Hydrophobic Modified Chitosan
HY-PEI	Hyperbranched Polyethylenimine Polymer
IFT	Interfacial Tension
LC_{50}	Median Lethal Concentration
LSC	Louisiana Sweet Crude
MW	Molecular Weight
NOAA	National Oceanic and Atmospheric Administration
OWR	Oil to Water Ratio
PAHs	Polycyclic Aromatic Hydrocarbons
PAMAM	Polyamidoamine
PBS	Phosphate Buffered Saline
SARA	Saturate, Aromatic, Resin, and Asphaltenic
SPM	Suspended Particulate Matter

Symbols

θ	Contact Angle
a_o	Optimal surface area per head group
$A_{o/w}$	Oil-water interfacial area
CPP	Critical packing parameter

LIST OF SYMBOLS AND ABBREVIATIONS (CONTINUED)

D	Diffusion Constant
ΔP	Pressure Difference
E	Attachment Energy
g	Gravity
G	London dispersion force
η	Viscosity
k_B	Boltzmann Constant
kDa	Kilodalton
l_c	Critical chain length
R	Radius of Curvature
r	Separation distance between atoms or molecules
r_p	Particle radius
T	Temperature
v	Hydrophobilc chain volume
W_K	Mixing energy
ψd	ζ potential
ψo	Surface potential
z	Vertical distance
β	London dispersion constant
$\gamma_{o/w}$	Oil-water interfacial tension

1 INTRODUCTION

The Deepwater Horizon incident began on April 20, 2010 and released over 200 million gallons of crude oil to the Gulf of Mexico (AFP 2010), second only to the estimated 420 million gallons released during the Gulf War (Tawfiq & Olsen 1993). The release was greater than the 140 million gallons of the IXTOC 1 offshore well spill in 1979 (Patton *et al.* 1981), and far exceeded the 11 million gallons of the 1989 Exxon Valdez spill off the coast of Alaska and the 4.3 million gallons of the 1969 Santa Barbara spill off California's coast (C&EN 2010). In addition to these major individual blowouts, an estimated 134 million gallons of oil was spilled collectively between 1990 and 1999 in the US, mostly from transport (ships and pipelines) and fixed facilities (Etkin 2001). It could be argued that oil spills are a part of "normal" petroleum industry operations.

During the Deepwater Horizon incident it was apparent that there was a lack of knowledge about how to deal with a release of that magnitude. Not only were engineers uncertain about how to stop the flow and collect the spilled oil, but the effects of dispersant use were not clearly understood. Decision makers were uncertain as to what extent the dispersants would be effective at breaking up the oil and they were even less certain of the environmental consequences of such large-scale use.

Due to the unprecedented nature of the spill, BP along with the U.S. Coast Guard and the Environmental Protection Agency decided to try the first subsea injection of chemical dispersants directly at the source. Over 700,000 gallons of chemical dispersants were sprayed directly onto the gushing oil at the wellhead in an attempt to keep some of the oil under the water surface. The dispersant use was intended to facilitate the biodegradation of the spilled oil by microbes to ultimately mitigate the shoreline impacts on fisheries, wetlands and other sensitive

environments. The National Oceanic and Atmospheric Administration (NOAA) estimated that over 400,000 barrels of the spilled oil were dispersed underwater in the form of oil plumes and small oil droplets.

Oil dispersion makes the oil more available to subsurface species where it can have a toxic effect. Corexit 9500 (hereafter referred to simply as Corexit) had a 96-hr median lethal concentration (LC_{50}) of 25.2 ppm for *Menidia beryllina*, a small fish that is found in estuaries of the Gulf (C&EN 2010). The 96-hr LC_{50} of No. 2 fuel oil is 10.7 ppm, but a mixture (1:10) of Corexit and No. 2 fuel oil is 2.61 ppm, ten times the toxicity of the dispersant alone. Later testing on Louisiana Sweet Crude (LSC) oil showed that the combination of Corexit with LSC was slightly less toxic than the LSC alone, but the oil toxicity was not significantly reduced by the dispersant (Hemmer, M. J., Barron, M. G., and Greene 2010). A more environmentally friendly dispersant would be one that effectively breaks up crude oil and produces a dispersed mixture that is significantly less toxic than the oil itself.

Previous investigations (Nisato *et al.* 2000; Lin *et al.* 2005; Maiti & Goddard 2006; Chen *et al.* 2007) have shown that dendrimers, such as poly (amido amine) (PAMAM) and poly (propyleneimine) are capable of encapsulating PAHs, inorganic solutes, and metal cations and anions, and then reversibly releasing the contaminant load upon changing the solvent pH and electrolyte strength or by a UV trigger (Diallo *et al.* 1999, 2007*b*, 2008; Arkas *et al.* 2003).The hydrophobic interior of the dendritic polymers, usually available at neutral pH, is especially suitable for the binding of hydrocarobons through hydrophobic, complexation and van der Waals interactions. The surface charge of the dendritic polymers, especially at low to neutral pH, affords them excellent solubility.

In previous study, our collaborators examined the interaction of poly(amidoamine) dendrimers and hyperbranched poly(ethyleneimine) polymers with model linear and polyaromatic hydrocarbons and found that both dendritic polymers had a strong ability to host polyaromatic hydrocarbons and linear compounds (Bhattacharya *et al.* 2013). Our objective for this study was to take the previous knowledge gained from work with model compounds and determine if those data are applicable to actual oil samples obtained from Gulf of Mexico oil production.

2 LITERATURE REVIEW

2.1 Oil spill dispersants

2.1.1 Definition of oil spill dispersants

Dispersants are chemical mixtures that break up oil from the surface and help it move into the water column by modifying the characteristics of the oil slick. Dispersants do not actually change the oil chemical structure, but coat the surfaces of the droplets to increase their solubility in water (Lessard & DeMarco 2000). Dispersants actually do not reduce the total mass of oil but accelerate oil's natural removal process by promoting the oil dissolution into the water column. The key for dispersant accelerating oil entrance into the water column is reducing the oil-water interfacial tension. Interfacial tension is a free energy that exists between two immiscible phases (e.g. oil and water), which is associated with the contact areas between these two phases. When the energy of waves in the ocean is introduced, the oil slick on the sea surface breaks up into small oil droplets which increases the oil-water interfacial area and interfacial tension. Dispersants are applied to reduce the oil-water interfacial tension and promote formation of smaller oil droplets. These small oil droplets then transport into the water column followed by biodegradation (NRC 2005).

2.1.2 Components of oil spill dispersant

In a review by Fiocco & Lewis (1999), it was explained that dispersants are usually not made up of just one component. Surfactants are one of the key components used, but solvents and other additives are also present and have a function in the dispersant properties. Additives are present for many purposes, such as improving the dissolution of the surfactants into an oil slick and increasing the long term stability of the dispersant formulation (Fiocco & Lewis 1999). Solvents are added to increase the solubility of surfactants and decrease the viscosity of the

dispersant mixture. By adjusting to a suitable viscosity, solvents help surfactants penetrate the oil slick and diffused to the oil-water interface (Brochu *et al.* 1986).

Surfactants typically are amphiphilic compounds that contain both hydrophilic groups and lipophilic groups in one molecule. Surfactants reduce the oil-water interfacial tension by residing at the oil-water interface with hydrophilic groups towards to water phase and lipophilic groups interacting with oil phase. Usually the oil compatible part of the surfactants contains hydrocarbons that are either branched linear or aromatic; these typically have similar structures from one surfactant type to another; however, the hydrophilic groups have more variability in structure among different surfactants (NRC 2005).

2.1.3 Characteristics of surfactants

Surfactants are usually classified into two categories according to their hydrophilic groups, ionic surfactant and non-ionic surfactant (Brochu *et al.* 1986). Non-ionic surfactants do not carry apparent ionic charge; many long chain alcohols are examples. Ionic surfactants have three subtypes, anionic, cationic and amphoteric. Anionic surfactants contain anionic functional groups in the water compatible part, such as sulfate and phosphate esters. Cationic surfactants carry cations in hydrophilic groups, either pH dependant (e.g. primary and secondary amines) or permanent (e.g. quaternary ammonium cations). Amphoteric surfactants contain both anions and cations in the head group (e.g. cocamidopropyl betaine). Typically, the surfactant contains only one head and one tail in each molecule. Other interesting surfactants, for example, Gemini surfactants, which were found in the late 1980s and early 1990s, has two hydrophilic heads and two hydrophobic tails in one surfactant molecule (Schramm *et al.* 2003).

The dispersion ability of surfactants largely depends on their solubility in water and oil. Usually commercial dispersants are a mixture of several surfactants with different solubility in

water and oil. The hydrophile-lipophile balance (HLB) is used to characterize these different solubilities. The HLB scale is from 0 to 20 based on its chemical structure (see Table 2-1). At low HLB value, surfactants have only a few hydrophilic groups and tend to form water-in-oil emulsions where oil is the continuous phase and water drops are dispersed in it. In contrast, at high HLB value, surfactants have lots of hydrophilic groups and prefer to dissolve in water rather than oil and form oil-in-water emulsion (Brochu *et al.* 1986). This phenomena has been summarized as Bancroft's rule, "the phase in which an emulsifier is more soluble constitutes the continuous phase." Typically, commercial dispersants usually have surfactants with HLB value around 7 to 11 (Clayton *et al.* 1993). In addition to solubility, other properties also have impacts on dispersion ability. In Piispanen's study, it has been found that surfactants which can become charged in water solution would form an electrostatic double layer and stabilize the emulsion. Less water soluble surfactants with large hydrophobic groups which may result in high cohesive monolayer energy form a liquid crystal phase depositing on particle surfaces that stabilize oil-in-water emulsions (Piispanen 2002).

Table 2-1 Summery of HLB ranges and their applications (Tadros 2013).

HLB range	Application
3-6	Water in oil emulsifier
7-9	Wetting agent
8-18	Oil in water emulsifier
13-15	Detergent
15-18	Solubilizer

2.1.4 Application of chemical oil dispersant

Oil dispersants are applied to enhance entrainment of small oil droplets into the water column at lower energy input by reducing the interfacial tension between the oil and water (Lessard & DeMarco 2000). Entrainment of oil droplets into the water column requires energy for increasing the oil-water interfacial area, which is expressed as Equation 2-1.

$$W_k = (\gamma_{o/w})(A_{o/w}) \quad (2\text{-}1)$$

Here W_K is the mixing energy (g cm^2 s^{-2}), $\gamma_{o/w}$ is the oil-water interfacial tension (dynes cm^{-1}) and $A_{o/w}$ is the oil-water interfacial area (cm^2). Therefore, by reducing the oil-water interfacial tension, dispersants can introduce a larger amount of oil-water interfacial area at the same level of energy input (NRC 2005). However, without dispersant, large oil droplets on the size range of hundreds of microns form at the same level of energy input. These large oil droplets tend to coalesce and resurface unless introducing strong mixing energy (Li & Garrett 1998; Gong *et al.* 2014).

In order to characterize the effectiveness of dispersants, two parameters have been introduced, critical micelle concentration (CMC) and critical packing parameter (CPP). Micelle formation is one of the most important characteristic of surfactants, where several surfactant molecules gather together with their hydrophobic parts aggregating toward the non-polar phase while the hydrophilic groups of surfactants orient toward the water phase in order to reduce the free energy of surfactants (Khan & Shah 2008). CMC has a narrow range and is defined as the concentration of surfactants above which micelles form (Schramm *et al.* 2003). Below the CMC, the surfactant has a strong tendency to adsorb on oil-water interfaces and the interfacial tension drops dramatically. Above the CMC, the interfacial tension of oil-water interfaces remains constant as the concentration of surfactant increases and newly added surfactant molecules

combine into micelles (Torchilin 2001). The effectiveness of surfactants can be defined as the degree of interfacial tension decrease at critical micelle concentration, the lower the interfacial tension, the higher the effectiveness of surfactants (Clayton *et al.* 1993).

CPP is another important characteristic of surfactant micelles. It is defined as a geometric expression relating the hydrocarbon chain volume (v) and length (l) and the interfacial area occupied by the head group and does not take electrostatic and other long range forces into consideration (Israelachvili *et al.* 1976; Piispanen 2002).

$$\mathrm{CPP} = \frac{v}{l_c a_0} \quad \textbf{(2-2)}$$

Here a_o is the optimal surface area per head group, v is the hydrocarbon chain volume, l_c is the critical chain length. This equation is applicable to predict the shape of an aggregated structure, for example surfactants that form spherical micelles have a CPP less than 1/3 (Tadros 2009).

Besides chemical effectiveness of dispersants, operational effectiveness and hydrodynamic effectiveness are also important components of overall effectiveness for oil dispersion. Operational effectiveness is described as the probability of dispersant contact with an oil slick. Hydrodynamic effectiveness is defined as the transportation of dispersed oil droplets by convection and diffusion in sea currents (NRC 2005). In this study, we focus on the chemical effectiveness which is defined as the amount of oil dispersed into the water column by dispersants compared with the mass of oil remaining on the water surface (Fingas & Advisory 2002).

There are many factors that influence the dispersant effectiveness, such as the properties of crude oil, water temperature and pressure. Viscosity is one of the important characteristics of crude oil. It has been generally reported that increasing viscosity reduces dispersant effectiveness

since high viscosity can inhibit migration of surfactants to the oil/water interface and increases the shear energy to break up the oil slick into droplets (Clayton *et al.* 1993). Rewick et al. (1984) reported that temperature can affect the dispersant effectiveness through the following aspects: the kinetics of surfactant packing at the oil/water interface; diffusion of the surfactant through the oil slick; and solubilization differences between the polar and nonpolar ends of the surfactant molecules (Rewick *et al.* 1984). A decrease in temperature would also result in an increase in viscosity which exerts a diminishing effects on dispersant effectiveness. Studies confirm that low temperature has adverse effects on oil dispersion (Mackay & Hossain 1982). The effects of deep water conditions such as high pressure and low temperature, which were present in the BP Deepwater Horizon incident, remain unclear and need further exploring.

2.2 Oil water emulsion

2.2.1 Surface forces

The goal of this study is to disperse oil, which is essentially to make an oil-in-water emulsion. Understanding how emulsions can be formed requires knowledge about the interactions between water, oil, and dispersants.

There are three main forces between molecules. These have been explained in depth in many textbooks (e.g. Tadros 2013). The first force is called van der Waals, and there are three sub-types for this force: dipole-dipole interactions, dipole-induced dipole interactions, and London dispersion. London dispersion is considered the most important of the three sub-types of van der Waals forces. They are caused by charge fluctuations as electrons move around atoms. There is a useful equation to describe these forces (Tadros 2013):

$$G = -\frac{\beta}{r6} \tag{2-3}$$

Here β is the London dispersion constant determined by the polarizability of atoms or molecules, r is the separation distance between atoms or molecules.

The second force is named electrostatic interaction which is also explained in detail in many papers and textbooks (e.g. Ivanov *et al.* 1999; Sjoblom 2005). Particles become charged in electrolyte solution by adsorption of ions or ionization of surface groups. This charged particle is then balanced by equivalent numbers of oppositely charged counter ions which tend to stay close to the particle by electrostatic attraction but also diffuse throughout the solution due to thermal energy (Ivanov *et al.* 1999). This is called the electrical double layer. It prevents particle aggregation or oil drop coalesce as a repulsion occur due to the overlap of diffuse layers when particles approach close to each other (Sjoblom 2005). Deryaguin, Landau, Verwey and Overbeek established the famous DLVO theory by a combination of van der Waals attraction and double layer repulsion.

Steric repulsion also plays an important role in molecular interactions. Steric repulsion often occurs in non-ionic surfactants or polymer stabilized systems. When two polymer coating surfaces approach to each other, the repulsion osmotic force occurs due to the compressing of hydrophilic chains. This steric repulsion stabilizes the colloids in water solution (Israelachvili 2011).

2.2.2 Breakdown process and stabilization mechanisms

The stability of a disperse system is characterized by a constant behavior in time of its basic parameters, namely, the dispersivity and the uniform distribution of the dispersed phase in the medium (Sjoblom 2005). Various breakdown processes are shown in Figure 2-1.

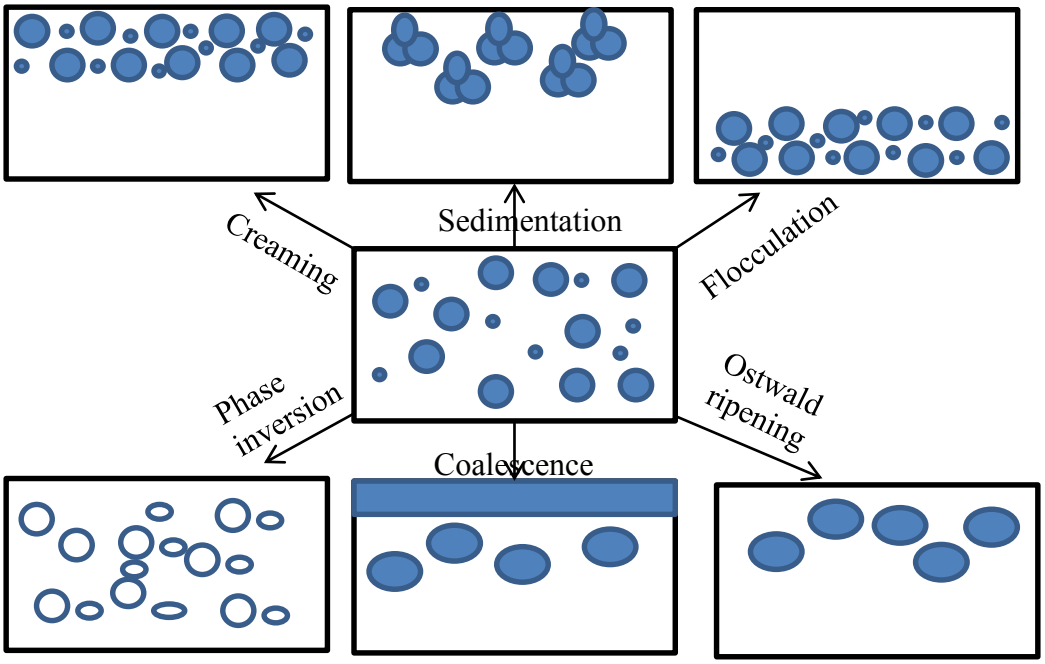

Figure 2-1. Schematic representation of the various breakdown processes in emulsions.

Among these breakdown processes, flocculation and coalescence are the main reasons for oil drop enlargement. Flocculation refers to the small oil drops clustered together to form the aggregation by van der Waals force. And this process leads to the increase of oil droplet size and probability of coalescence (Ivanov *et al.* 1999). Coalescence is described as two drops approach close to each other and form a thin liquid film between interfaces. This thin liquid film then ruptures and becomes sufficiently small, so small oil drops coalescence to one large oil drop (Chen 1985; Deshiikan & Papadopoulos 1995). Tadros pointed out two mechanisms to prevent coalescence: increasing either electrostatic repulsion or steric repulsion or both, and decreasing the oil drop size (Tadros 2009).

Nowadays, a number of discoveries and investigations are made in stabilization of oil droplets in a water column. Venkataraman & Tang (2013) found that adding biopolymer such as hydrophobic modified chitosan into commercially used dispersant (e.g., Corexit) can increase the efficiency of dispersant stabilizing the oil drops and reduce the use of chemical dispersants

(Figure 2-2). This may result from the increasing electrostatic and steric repulsions created by biopolymers which form barriers to prevent coalescence between oil drops (Venkataraman & Tang 2013).

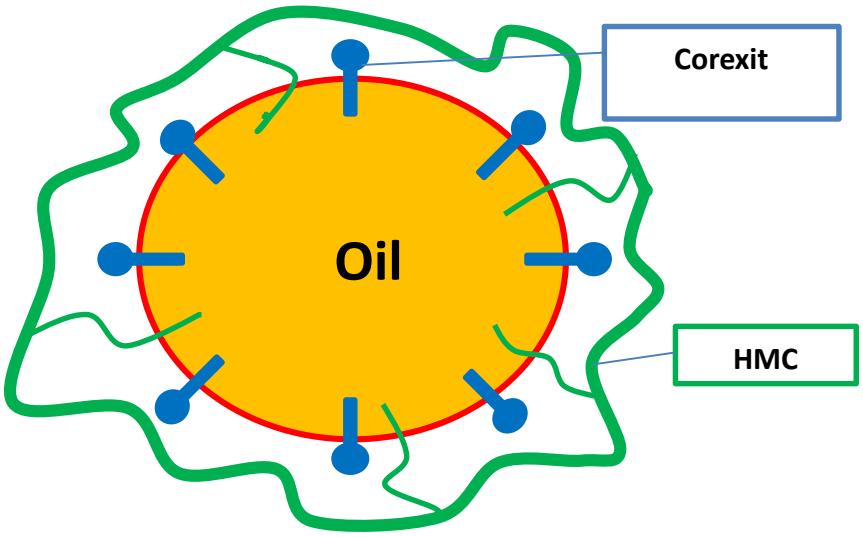

Figure 2-2 Schematic showing hydrophobically modified chitosan (HMC) molecules stabilizing dispersed oil droplets by anchoring the covalently attached alkyl groups at the oil−water interface and forming a protective layer around the oil droplet (Venkataraman & Tang 2013)**.**

Ye *et al*. (2013) discovered that protein coating nanoemulsion droplets (average size around 150 nm) can work as an emulsifier to stabilize oil (n-hexadecane)-in-water emulsions. These nanoemulsion droplets can stabilize the emulsion at very low concentrations and the size of emulsion depends on the nanodroplets concentration (Ye *et al.* 2013).

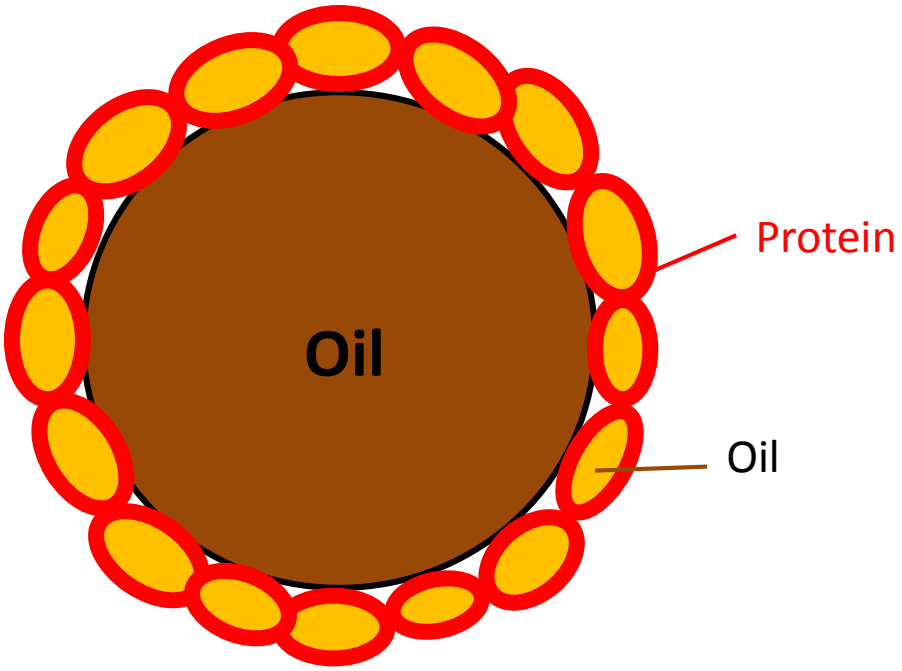

Figure 2-3 Schematic showing oil drop stabilized by protein-coated nanoemulsion drops (Ye *et al.* 2013).

Folter et al demonstrated that water-insoluble proteins, corn protein zein as representation, are natural and biocompatible dispersants that effectively stabilize oil-in-water emulsions. This Pickering emulsion by corn protein zein prefers a condition of high pH and low ion strength (de Folter *et al.* 2012). Another particle stabilized oil-in-water emulsion has been examined by Saha & Nikova (2013). They found that carboxyl-terminated carbon black (CB) has great adsorption capacity and ability to stabilize the emulsion which makes these particles a viable alternative to commercial dispersants (e.g. Corexit) in dealing with oil spills (Saha & Nikova 2013).

2.3 Pickering emulsion

Pickering emulsion was named after Pickering who first found that small colloid particles can remain at the oil-water interface where they minimize the system free energy and form a

rigid barrier to prevent oil drop coalescencence (Pickering 1907; Aveyard *et al.* 2003). An equation illustrates the mechanism of Pickering emulsion, Equation 2-4.

$$E = \pi {r_p}^2 \gamma_{o/w} (1 \pm \cos\theta)^2 \quad (2\text{-}4)$$

Here r_p is the radius of the particle, $\gamma_{o/w}$ is the oil-water interfacial tension, θ is the contact angle (Binks 2002). Besides the size and contact angle of particle, the particle stability is also influenced by hydrophobicity, shape and wettability (Tadros & Vincent 1983). Binks predicted that "Janus" particles which have two surface regions of different wettability would better stabilize the oil emulsion than homogenous particles for the combination of Pickering effects and amphiphilicity of surfactants would results in considerably increasing surface activities (Binks & Fletcher 2001; Glaser *et al.* 2006).

2.4 Dendritic polymers and applications

Dendritic polymers are highly branched spherical three dimensional macromolecules which can be divided to two subtypes, dendrimer and hyperbranched polymer. Dendrimers have highly uniform, monodisperse structures which are composed of a central core, repeating units and terminal functional groups (Seiler 2002). Unlike dendrimers, hyperbranched polymers have a polydispersed, irregular branching structure. Dendrimers are usually prepared in multistep syntheses with protection/deprotection procedures, with addition chemistry and purifications at each step. Hyperbranched polymers, in contrast, can be prepared in a one-step procedure. The details are explained in many papers for dendrimers (Tomalia *et al.* 1985; Matthews *et al.* 1998; Farrington & Hawker 1998) and for hyperbranched polymers (Kim 1998; Sunder *et al.* 1999).

The properties of dendritic polymers depend on both polymer structure and environmental conditions such as pH, temperature and ion strength. The intrinsic viscosity of the

dendrimer has a well-observed bell-shaped curve with molecular weight. For example, the viscosity of PAMAM increases until generation four and decreases with further increasing molecular weight (Cai & Chen 1998; Bhattacharya *et al.* 2013). The viscosity of hyperbranched polymers depends on the degree of branching. At low branching level, the viscosity is determined by chain entanglement while at high branching level, the viscosity of hyperbranched polymers behaves similarly to dendrimers (Farrington & Hawker 1998).

Dendritic polymers are more soluble in water compared with the analogous linear polymers. And solubility is largely determined by the surface groups. For example, dendrimers with very hydrophobic interior can be adjusted to water soluble by introducing hydrophilic surface groups into the surface (Inoue 2000).

The hydrodynamic size of dendritic polymers varies with solvent properties and surface groups. It has been found that dendrimers with carboxylic acid surface groups were found larger in neutral pH and shrank at acidic pH, while dendrimers with the same interior structure but amino terminal group expanded at acidic pH and contracted at basic pH (Newkome *et al.* 1993; Young *et al.* 1994). Studies by Murat and Grest (1996) and Stechemesser and Eimer (1997) suggest that the size of dendrimers is a function dependent on a one third exponental of monomer number (Murat & Grest 1996; Stechemesser & Eimer 1997).

One of important characteristics of dendritic polymers that should be carefully examined is the biocompatibility. The success of dendrimer application to oil spills will depend on whether the dendrimers or oil-dendrimer complexes can be taken up and biodegraded by microorganisms in the subsurface. In one review paper (Lee *et al.* 2005), it has been reported that PAMAM dendrimers are hydrolytically degradable only under harsh conditions because of their amide backbones, and the process is slowly under physiological temperature. Dendrimers with

polyester backbones are nontoxic, natural metabolities (Grinstaff 2002). Another study found that dendritic polymers with thiol-reactive disulfides in their branches should have the ability to cleave under reducing conditions in cells (Zhang *et al.* 2003). And if the chains of dendrimers contain enzyme substrates they would add an extra pathway for biodegradation (Seebach *et al.* 1996).

Another significant property of dendritic polymers affecting their application in oil spills is light sensitivity. When the polymers are applied at the sea surface, the oil polymer complexation and polymer itself may remain for a certain time and be exposed to sunlight. It has been reported in a biomedical paper (Lee *et al.* 2005) that dendrimers can be prepared for photolysis. The mechanisms of dendrimer photolysis are variable, including Dendrons released from the core, peripheral groups cleaved, or the entire molecule degraded into identical small fragments under ultraviolet irradiation (Smet *et al.* 2000; Watanabe *et al.* 2000; Grinstaff 2002; Amir *et al.* 2003). Recent studies show that dendritic polymers such as PAMAM and PPI can encapsulate polycyclic aromatic hydrocarbons, metal cations and anions, as well as other inorganic compounds. By adjusting the solution pH, electrolyte strength or using UV light, the dendritic polymer can reversibly release the compounds it encapsulated (Arkas *et al.* 2003; Meijer & Van Genderen 2003; Diallo *et al.* 2007*a*, 2008).

There are many applications for dendritic polymers. Dendritic polymers have been employed as building blocks for the self-assembly of several larger nano- and mesoscopic structures, micelle aggregates, and discrete hydrogen-bonded superstructures (Zeng & Zimmerman 1997). Dendrimers are also considered as promising interfacial agents due to the large numbers of controllable surface functionalities, well-defined architecture and chemical

stability. Cooper and coworkers demonstrated that the encapsulation ability of dendritic polymers can be applied to the area of extraction chemistry (Cooper *et al.* 1997)

Compared with dendrimers, hyperbranched polymers are easier to synthesize and produce in large scale. It has been reported that hyperbranched polymers could be utilized as rheology modifiers, adhesives, coatings, and additives in process engineering. They can also be applied for the accelerated processing of commodity polymers (Kim & Webster 1992; Hult *et al.* 1999; Seiler 2002). Among these, one of the interesting studies shows dendritic polymers could be alternative oil spill dispersant that are both effective and biocompatible (Geitner *et al.* 2012). In the latter paper it was found that both poly (amidoamine) dendrimers and hyperbranched poly(ethyleneimine) polymers exhibited a strong and comparable hosting/dispersion capacity for the polyaromatic hydrocarbon phenanthrene and the linear hydrocarbon hexadecane ($C_{16}H_{34}$) (Geitner *et al.* 2012).

A recent paper (Bhattacharya *et al.* 2013) from our collaborators thoroughly reviewed the physicochemical properties of dendritic polymers and introduced the applications in the environmental and biological field. It was reported that dendritic polymers can be applied in antifouling, oil spill, dendrimer-fullerenol assembly and dendrimer-gold nanowires for copper sensing. The high biocompatibility, hosting capacity, and low toxicity makes dendrimers perfect candidates in medical applications. Besides, compared to globular proteins that are essentially folded structures therefore susceptible to denaturation by temperature, light and pH, dendritic polymer has a covalently fixed nature with well-defined interiors and homogenous surface providing a precise function.

The manufacturing price of dendrimers is much higher than hyperbranched polymers and Tween 80 which is one of the key active surfactants in Corexit. From Sigma-Aldrich, the unit

price for PAMAM generation 4 is around $1000 per gram; the unit price for HY-PEI is $1 per gram; and unit price for Tween 80 is $0.2 per gram. So from a view of mass application in oil spill, the Tween 80 is much cheaper than PAMAM dendrimers; however, HY-PEI is still a good option because is only $1 per gram and more biocompatible. Also, these prices would certainly change once mass production is implemented for HY-PEI if there were a market for oil spill dispersion or other applications. Tween 80 has already been on the market for many years, so there is a great deal of competition among suppliers and large-scale production techniques are well established.

2.5 Dispersant performance evaluation

2.5.1 Chemical effectiveness test

Oil dispersant effectiveness includes three components: operational effectiveness, chemical effectiveness and hydrodynamic effectiveness. Operational effectiveness evaluates the efficiency of dispersant application methods and hydrodynamic effectiveness examines transportation of dispersed oil droplets by convection and diffusion in natural ocean conditions. Our study is focus on whether the dendritic polymer can disperse crude oil and what are the mechanisms of dispersion, such as the oil-polymer chemical interactions. The focus of this section of the literature review is on the experimental methods to evaluate dispersant effectiveness.

Chemical effectiveness tests range from bench-scale to large scale field trials (NRC 2005). Among these, bench scale experiment are a useful tool to compare dispersant effectiveness of different products (Venosa *et al.* 2002). The effectiveness is defined as the fraction of oil dispersed in a water column. There are many factors that could affect the

effectiveness such as physical and chemical characteristics of crude oil; oil:water ratio; dispersant:oil ratio; salinity; temperature; physical and chemical properties of dispersant; methods of applying the dispersant to oil; energy input; settling time; and method used to measure effectiveness (Sorial *et al.* 2004*a*; NCR 2005; Chandrasekar *et al.* 2006).

The physical characteristics (such as viscosity and density) and chemical composition (such as aromatic, aliphatic and asphaltic hydrocarbon concentration) are important because they change greatly among oil with different sources. These characteristics also change with oil weathering after a spill (Mukherjee & Wrenn 2011).

The method of applying the dispersant is also an important factor that influences the effectiveness. This is because the dispersant should first penetrate the oil slick and reach to the oil-water interface before it disperses the oil (Sorial *et al.* 2004*a*). Typically there are three methods for applying the dispersant: premix the oil and dispersant before the test (which we used in some effectiveness tests for Corexit); premix the dispersant with water before the test (which we used in our interfacial tension measurements); and mix the dispersant with oil at the oil-water interface as part of the testing procedure (which we used in most of our effectiveness tests).

The dispersant to oil ratio (DOR) and oil to water ratio (OWR) are critical factors that affect dispersion effectiveness. Several studies show that there is a direct relationship between DOR and dispersion efficacy (Fingas *et al.* 1989). The DOR of 1:25 and 1:50 are commonly used, but smaller and larger DORs are used in different studies. The OWR also varies over a large range, from 1:1 to 1:120,000 (Fingas *et al.* 1989). The OWR affects the extent of partitioning. When OWR is high, more dispersant is associate with oil and droplet formation is promoted. On the other hand, high OWR can also reduce the effectiveness by increasing the rate of oil droplet coalescence.

Energy dissipation or mixing rate is one of the most important factors in effectiveness testing. Energy is required for creating a new interfacial area when an oil slick breaks up into dispersed oil droplets. Increasing energy input will result in the formation of smaller oil droplets which are more stable, having a reduced tendency to resurface (Kaku *et al.* 2006).

2.5.2 Interfacial tension and pendant drop method

Interfacial tension is usually used to measure cohesive energy between immiscible phases; it is one of the important parameters that characterizes the dynamic properties of liquid adsorption layers. There are many methods to measure the interfacial tension, including the Du Nouy ring method, Wilhelmy plate method, spinning drop method, drop-weight method, etc. In this study, we used the pendant drop method, where interfacial tension is determined by the axisymmetric drop shape analysis (ADSA) technique. The ADSA technique is considered by some to be an advantageous method for its accuracy, simplicity, and versatility (Jennings & Pallas 1988; Cheng & Neumann 1992). It is also very suitable for automatic computer implementation by combination with video frame image analysis (Girault *et al.* 1984).

Interfacial tension measurement by drop shape analysis is based on the classical Young-Laplace equation.

$$\Delta P = \gamma(\frac{1}{R1} + \frac{1}{R2}) \quad (2\text{-}5)$$

Here ΔP (Pa) is the pressure difference across the drop interface, γ (mN/m) is the interfacial tension and R1 and R2 (m) are the radii of curvature (Woodward 1948). If no external forces are present other than gravity, the difference in pressure is linear to the ascending forces, as shown in Equation 2-6.

$$\Delta P = \Delta P_0 + (\Delta\rho)gz \quad (2\text{-}6)$$

Here ΔP_0 is the pressure difference at a certain datum plane, $\Delta\rho$ is the density difference of two bulk phases, g is the gravity and z is the vertical distance between the given point and the datum plane. By combining equation Equation 2-5 and Equation 2-6 we obtain Equation 2-7.

$$\frac{d\theta}{dS} = \frac{2}{Ro} + \frac{(\Delta\rho)g}{\gamma} Z - \frac{\sin\theta}{X} \tag{2-7}$$

For any pendant drop where the densities of two liquid phases in contact are known, the interfacial tension can be calculated by iterating the equations above (Kruss company 2012). Figure 2-4 shows a schematic of the pendant drop method with symbols.

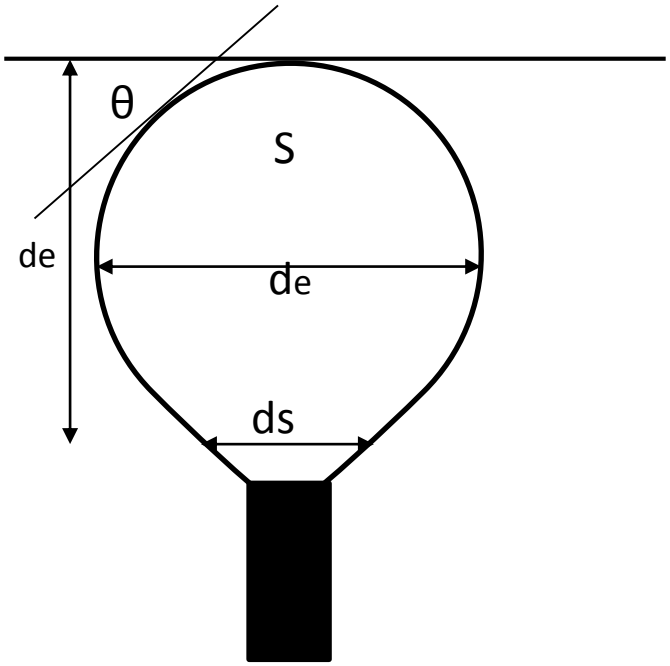

Figure 2-4 Schematic of the pendant drop method.

A typical pendant drop apparatus contains three parts: a transparent illuminating cell, a light and camera system, and an image collecting and analysis system. The software analyses the image in four steps. First, it captures and digitalizes the drop image. Second, the drop shape is extracted and the important parameters are measured for calculation of interfacial tension, like the radius of curvature at the apex. Third, the interfacial tension is calculated and experimental data points are compared with theory.

When surfactants are present in the fluid, it usually takes a relatively long time to ensure stability. Video is taken for recording the changing interfacial tension as the drop ages. If no dispersant is present a more stable measurement can be taken (as long as there is little vibration) but with crude some small-molecule volatile compounds could be leaving and causing variation in drop shape over time.

The pendant drop method has been widely used in many experiments. Glaser *et al.* (2006) used the pendant drop method to show that the amphiphilicity derived from the Janus character of the particles under study led to a significantly higher interfacial activity compared to that of the respective homogeneous particles of the same size (Glaser *et al.* 2006). Morais (2006) used the pendant drop method to measure the surface tension of molten polymers (polyvinylbutyral) at temperatures ranging from 240℃ to 260℃ (Morais 2006). Reichert and Walker (2013) measured surfactant adsorption dynamics to the oil−aqueous interface for a range of surfactant concentrations with the pendant drop technique (Reichert & Walker 2013).

2.5.3 Dynamic light scattering

Dynamic light scattering (DLS) is a typical method to measure particle size distribution of diluted suspensions ranging from around 2 nm to 2 μm. DLS has the advantage of being rapid and simple with a solid statistical foundation through measuring large numbers of particles per experiment (Sjoblom 2005).

DLS is based essentially on two assumptions. The first is that the particles are in Brownian motion and we use the probability density function,

$$\mathrm{P}(\mathrm{r},\mathrm{t}|0,0) = (4\pi\,\mathrm{Dt})^{-\frac{3}{2}} \exp\left(-r^2/4\mathrm{Dt}\right) \qquad \textbf{(}2\text{-}8\textbf{)}$$

Here D is the diffusion coefficient. The second assumption is that the particles in suspension are spherical and small compared to the molecular dimensions so we can apply the Stokes-Einstein relation.

$$D = k_B T/6\pi\eta a \quad (2\text{-}9)$$

Here k_B is the Boltzmann constant, *a* refers to the radius of the particles, T is the temperature in Kelvin and η is the viscosity of the solvent. The speed of Brownian motion is determined by both temperature and particle size, therefore temperature control is important for accurate size measurement (Sjoblom 2005).

To measure the diffusion speed, the speckle pattern produced by illuminating the particles with a laser is observed. The scattering intensity at a specific angle will fluctuate with time, and this is detected using a sensitive avalanche photodiode detector (APD). The intensity changes are analyzed with a digital autocorrelation which generates a correlation function. This curve can be analyzed to give the size and the size distribution (brochure from Malvern).

DLS measurements are widely used in studies of polymers, food emulsions, drug delivery vectors, and coagulation rates in colloidal systems. Honary *et al* (2014) optimized particle size and encapsulation efficiency of vancomycin nanoparticles prepared from chitosan (Honary *et al.* 2014). Shpigelman and co-workers used the DLS technique to find that nanoparticles about 10 nm in size, which is marginally larger than those of the pure protein (about 7 nm), makes beverages more clear (Shpigelman *et al.* 2014). Macedo *et al.* (2014) designed and characterized a rutin-loaded nanoemulsion and determined the release profile of the drug in vitro by DLS (Macedo *et al.* 2014). DLS has also been applied in determination of Ostwald ripening rates and destabilization phenomena in aqueous phase (Noor El-Din *et al.* 2013). These are just a few of a myriad of studies using DLS, since it is a well-established laboratory technique.

2.5.4 Coulter counter

The Coulter counter method is based on the principle discovered by Wallace H Coulter in the late 1940s (Coulter 1953). The Coulter principle states that particles pulled through an orifice, concurrent with an electric current, produce a change in impedance that is proportional to the volume of the particle traversing the orifice. In a Coulter counter, a small aperture on the wall is immersed into a container that has particles suspended in low concentration electrolyte solution. Two electrodes are placed: one in front and one behind the aperture, and a current path is provided by the electrolyte. When an electric field is applied the aperture creates a ‘‘sensing zone.’’ As a particle passes through the aperture, a volume of electrolyte, equivalent to the immersed volume of the particle is displaced from the sensing zone. This causes a short-term change in the impedance across the aperture. This change can be detected as a voltage pulse and its height is proportional to the volume of the sensed particle, see Figure 2-5 (Zhang *et al.* 2009). Due to its simplicity, high sensitivity and reliability, it is a widely used method in many areas including medical and biology fields, such as counting and analysis of blood cells (Bowers *et al.* 2013), protein (Kulp *et al.* 2004), and viruses (Wahl-Jensen *et al.* 2007). The Coulter counter is also a very useful technique for size distribution analysis in emulsions and suspensions (Walstra & Oortwijn 1969). Sterling *et al*. investigated the thermodynamics and kinetics of crude oil drop coalescence in saline waters using a Coulter counter (Sterling *et al.* 2004). Reynolds *et al.* found that a Coulter counter could provide a higher resolution of particle size distribution than laser in-situ scattering and transmissometry (LISST), characterizing the number of small particles more accurately than LISST. In Reynolds’ case the Coulter counter was also better than the FlowCAM flow cytometer and imaging system (Reynolds *et al.* 2010).

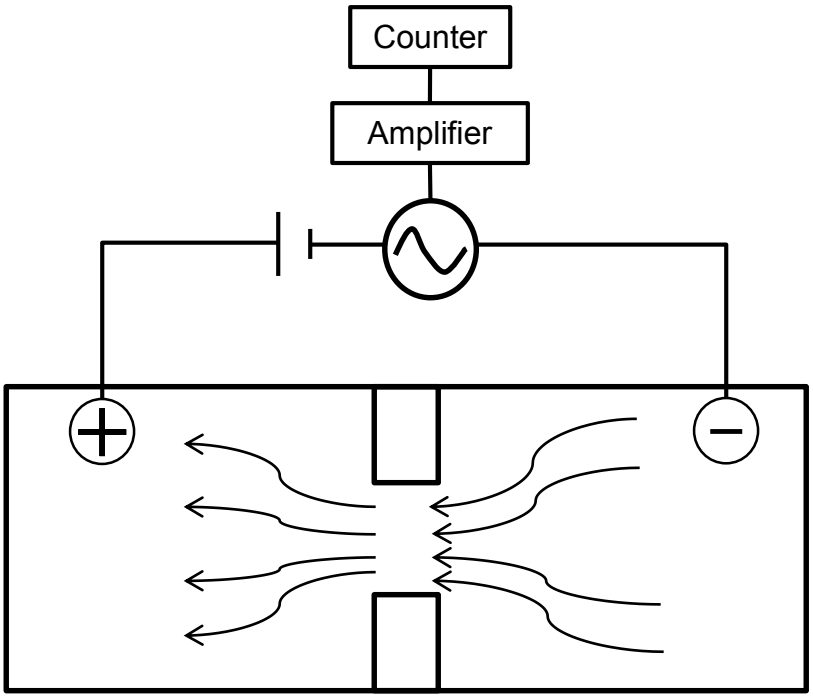

Figure 2-5 Schematic of Coulter counter.

3 OBJECTIVES

There are three ojectives of this research:

1) Develop methods to adequately characterize the oil-dispersion effectiveness of dendritic polymers. There are many effectiveness tests reported in the literature, with different methods resulting in variable data, leading to different conclusions. We need a solid technique that can provide high reproducibility.
2) Test and verify the hypothesis that dendritic polymers can disperse crude oil. In previous studies our collaborators demonstrated that the dendritic polymers could encapsulate model compounds (linear and polyaromatic hydrocarbons). In this study, we aim to explore the dispersion capacity of dendritic polymers in association with crude oil rather than model compounds.
3) Gain a fundamental understanding of the interactions of dendritic polymers with crude oil. Whether or not the dendritic polymers have high dispersion capacity on crude oil, we would like to figure out the mechanism of oil polymer interactions which may benefit the future development of dispersant materials.

4 EXPERIMENTAL METHODOLOGY

4.1 Materials

4.1.1 Artificial seawater

Oil was dispersed in artificial seawater which was prepared by dissolving 35 g of sodium chloride (Sigma) and 0.2 g of sodium bicarbonate (EMD) in 1 L of ultrapure deionized water. The artificial seawater was filtered through a 0.2 μm membrane filter (Millipore, Isopore membrane filters, 0.2 μm GTTP) after adjusting pH to between 7.9 and 8.1with a pH meter. Filtration removed suspended particles that could interfere with oil droplet measurement. Artificial seawater was stored in glass bottles at room temperature (22 ℃). Sodium chloride is used to simulate the typically salinity of seawater 35g/kg, and sodium bicarbonate is applied to adjust pH to 8 which is a common value for seawater.

4.1.2 Crude oil

Crude oils are mixtures of hydrocarbons ranging from small volatile contents to very large, nonvolatile compounds (Speight 2006). Crude oil contains numerous compounds of different sizes and classes. Some analysts have identified up to 17,500 compounds in an oil (Fingas 2011). Besides hydrocarbons, crude oils also contain varying amounts of sulfur, nitrogen, oxygen, mineral salts and trace metals such as nickel and chromium. A well-accepted method of classification is by saturates, aromatics, resins, and asphaltenes (SARA). Aromatic compounds include at least one benzene ring which is very persistent and can have toxic effects on the environment. The common smaller aromatic compounds found in oil are often referred to as BTEX, or benzene, toluene, ethyl-benzene, and xylenes. The larger aromatic compounds containing at least two benzene rings are referred to as PAHs, which make up 0 to 60% of the

composition of oil. In this study, we used Louisiana light sweet crude oil obtained from a commercial oil company and stored in a plastic barrel within a hood at room temperature (22 ℃). Table 4-1 shows the composition and properties of light crude oil.

Table 4-1. Typical composition and properties of light crude oil (Speight 2006)**.**

Composition (%)		Properties	
Saturates	55-99	Viscosity (mPa s at 15 ℃)	5-50
Aromatics	10-35	Density (g/mL at 15 ℃)	0.78-0.88
Polar Compound	1-15	Solubility in Water (ppm)	10-50
Metals (ppm)	30-250	API Gravity	30-50
Sulfur	0-2	Interfacial Tension (mN/m at 15 ℃）	10-30
		Pour Point (℃)	-40-30

4.1.3 Dispersant and dendritic polymers

Corexit (Nalco) is a commercially used oil dispersant which was applied in the 2010 Deepwater Horizon oil spill in the Gulf of Mexico. One key active ingredient in Corexit is sorbitan mono-(9Z)-9-octadecenoate (commonly known as Tween 80 or polysorbate 80), a nonionic surfactant commonly used in industry and consumer products. Another key ingredient is butanedioic acid, 2-sulfo- 1,4-bis (2-ethylhexyl) ester, sodium salt (1:1) (often referred to as dioctyl sodium sulfosuccinate [DOSS]), also a common surfactant in industry and consumer products. Other Corexit ingredients are listed on the Nalco website, as requested by the EPA (Nalco 2011). HY-PEI is an abbreviation for hyperbranched polyethylenimine polymers with a chemical structure of $(\text{-NHCH}_2\text{CH}_2\text{-})_x[\text{-N}(\text{CH}_2\text{CH}_2\text{NH}_2)\text{CH}_2\text{CH}_2\text{-}]_y$; x and y indicate the number of repeating units, which are variable for the materials used here. In this study five different molecular weight polymers 1.2, 1.8, 10, 70, and 750 kDa were used to examine the effect of polymer size on dispersant effectiveness. HY-PEI was supplied by Polyscience. With a similar interior structure and molecular weight as HY-PEI, dendrimers with various terminal groups

were examined to explore the effects of surface group and charge on dispersion efficiency. PAMAM dendrimers with different surface functional groups were also studied. G4-PAMAM-NH_2 with a molecular weight of about 14 kDa has an amino surface functional group and is positive in the working solutions used here, at about pH 8. According to Cakara & Borkovenc (2007) study, primary amine groups of PAMAM protonate in the first step at a pH of appximately 9.0 roughly, while the tertiary amine groups protonate in two well-separated steps at pH ≈ 6.4 and pH ≈ 3.5 (Cakara & Borkovec 2007). G4-PAMAM-OH, also with a molecular weight of 14 kDa has amidoethanol surface groups and has a nearly neutral charge around pH 8. G4-PAMAM-SA with molecular weight of about 21 kDa has succinamic acid surface groups and is negatively charged in aqueous solution (Ciolkowski *et al.* 2013).

4.2 Methods

4.2.1 Preliminary Experiments

4.2.1.1 Small vials test

Small vials refer to the 20 ml scintillation vials used in this series of tests. In experiment, we used 12 ml artificial seawater and 25 µl crude oil that is less than the chemical effectiveness test we describe later; thus, this section describes our method development for adequately characterizing the dispersion effectiveness of the polymers. In order to understand the factors that may affect effectiveness results, we tried different dispersant-oil ratios, mixing and settling time, sample collection methods, and sample preparation methods. The effectiveness test consisted of four steps: sample preparation, mixing and settling, sample collection and sample analysis. In sample preparation, we used non-premix and premixed methods to make the sample. For non-premix, oil was added to the water surface first then the dispersant working solution was added to the oil slick. For premix, oil was first mixed with the dispersant and then applied the

mixture to the water surface. Both methods are found in the literature (Sorial *et al.* 2004*b*; Mukherjee & Wrenn 2011) and here we evaluated the differences between them. Three dispersant to oil ratios (DORs) were examined in the small vials tests: 0.02, 0.04, and 0.08. DOR was calculated on a mass basis (for the small-vials tests and for the high-volume tests described later). Oil was added volumetrically to each sample and the oil mass was calculated using its density. The oil density is 0.83 g/ml which obtained by measuring the weight of certain volume of oil in balance. The polymer mass was calculated from working solutions which were prepared by directly weighing the appropriate mass of polymer stock solution as received from the manufacturer and correcting for the concentration reported on the bottles (99%, 99%, 30%, 30%, and 50% for the 1.2, 1.8, 10, 70, and 750 kDa materials, respectively). Volumetric measurement of the polymer stock solutions was not possible because of their high viscosity. The DOR values reported here are unitless, but can be interpreted as mass of polymer divided by mass of oil.

Effects of mixing and settling time were also considered in small vial tests. In this experiment, we used the non-premix method to prepare the sample and choose a DOR of 0.02. Three combinations were tested: mixing 24 h then settling 2 h, mixing 1h then settling 30 min, and mixing 30 min then settling 15 min.

Sample collection seemed have a significant influence on the effectiveness results in early tests, so a few collection methods were used. For small vial trials, the total amount of oil-water-polymer mixture was 12 ml, so the collected water sample containing dispersed oil (and not containing non-dispersed oil floating on the top of the sample) was less than 12 ml. One method that was used to collect the water was inserting a needle from the top, through the oil layer, to the bottom of the water column and aspirating a 3 ml water sub-sample. The other

method was to use a needle penetrating into the side of the plastic vials and extracting the 3 ml sub-samples from the bottom, as shown in Figure 4-1.

Figure 4-1. In some experiments, 3 ml water sub-samples with dispersed oil were extracted from the bottom of plastic vials using a needle penetrate through the vial.

For measuring the quantity of dispersed oil dichloromethane DCM was added to the sample and the oil was extracted from the water column for 30 minutes into the DCM. The DCM with extracted oil was placed in 200 µl aliquots into the wells of a 96 well plate and visible-light absorbance was measured at 340 nm. We related the absorbance data with the actual oil mass in the vials.. The fraction of oil dispersed into the water was quantified by comparison with measurements of the absorbance from whole-oil samples. Table 4-2 shows the experimental matrix of the small vial tests.

Table 4-2 Experiment matrix of small vial trials.

Experiment number	Sample Preparation	Materials	DOR	Mixing/ Settling (hr)	Sample collection
1	Non-premix	HY-PEI 10 kDa	0.02	24 / 2	Top insertion
2	Non-premix	HY-PEI 10 kDa	0.02	1 / 0.5	Top insertion
3	Non-premix	HY-PEI 10 kDa	0.02	0.5 / 0.25	Top insertion
4	Non-premix	HY-PEI 10 kDa	0.02	0.5 / 0.25	Top insertion
5	Non-premix	HY-PEI 10 kDa	0.04	0.5 / 0.25	Top insertion
6	Non-premix	HY-PEI 10 kDa	0.08	0.5 / 0.25	Top insertion
7	Non-premix	Corexit	0.02	0.5 / 0.25	Top insertion
8	Non-premix	Corexit	0.04	0.5 / 0.25	Top insertion
9	Non-premix	Corexit	0.08	0.5 / 0.25	Top insertion
10	Non-premix	G4-PAMAM-NH2	0.02	0.5 / 0.25	Top insertion
11	Non-premix	G4-PAMAM-NH2	0.04	0.5 / 0.25	Top insertion
12	Non-premix	G4-PAMAM-NH2	0.08	0.5 / 0.25	Top insertion
13	NA*	NA*	NA*	0.5 / 0.25	Top insertion
14	Non-premix	HY-PEI 1.2 kDa	0.02	0.5 / 0.25	Top insertion
15	Non-premix	HY-PEI 1.8 kDa	0.02	0.5 / 0.25	Top insertion
16	Non-premix	HY-PEI 10 kDa	0.02	0.5 / 0.25	Top insertion
17	Non-premix	HY-PEI 70 kDa	0.02	0.5 / 0.25	Top insertion
18	Non-premix	HY-PEI 750 kDa	0.02	0.5 / 0.25	Top insertion
19	Non-premix	Corexit	0.02	0.5 / 0.25	Top insertion
20	Non-premix	HY-PEI 1.2 kDa	0.02	0.5 / 0.25	Side penetrate
21	Non-premix	HY-PEI 1.8 kDa	0.02	0.5 / 0.25	Side penetrate
22	Non-premix	HY-PEI 10 kDa	0.02	0.5 / 0.25	Side penetrate
23	Non-premix	HY-PEI 70 kDa	0.02	0.5 / 0.25	Side penetrate
24	Non-premix	HY-PEI 750 kDa	0.02	0.5 / 0.25	Side penetrate
25	Non-premix	Corexit	0.02	0.5 / 0.25	Side penetrate
26	Premix	HY-PEI 1.2 kDa	0.02	0.5 / 0.25	Top insertion
27	Premix	HY-PEI 1.8 kDa	0.02	0.5 / 0.25	Top insertion
28	Premix	HY-PEI 10 kDa	0.02	0.5 / 0.25	Top insertion
29	Premix	HY-PEI 70 kDa	0.02	0.5 / 0.25	Top insertion
30	Premix	HY-PEI 750 kDa	0.02	0.5 / 0.25	Top insertion
31	Premix	Corexit	0.02	0.5 / 0.25	Top insertion
32	Premix	HY-PEI 1.2 kDa	0.02	0.5 / 0.25	Side penetrate
33	Premix	HY-PEI 1.8 kDa	0.02	0.5 / 0.25	Side penetrate
34	Premix	HY-PEI 10 kDa	0.02	0.5 / 0.25	Side penetrate
35	Premix	HY-PEI 70 kDa	0.02	0.5 / 0.25	Side penetrate
36	Premix	HY-PEI 750 kDa	0.02	0.5 / 0.25	Side penetrate
37	Premix	Corexit	0.02	0.5 / 0.25	Side penetrate

NA*= none applicable

4.2.1.2 Calibration curve

Calibration curves were developed to transcribe the absorbance data to actual oil mass. Five volumes of oil (10 µl, 15 µl, 20 µl, 25 µl and 30 µl) were separately added to 40 ml artificial seawater in plastic centrifuge tubes, then rotated for 30 min and left to stand for 15 min. Oil was extracted from the water phase by adding 10 ml DCM then placing the extraction in a 96 well plate followed by examining absorbance at a wavelength of 340 nm. Also, five concentrations of oil in DCM solution (0.125, 0.25, 0.5, 1, 2 µl oil/ ml DCM) were prepared and measured via spectrophotometer (also at 340 nm, as above).

4.2.2 Higher volume chemical effectiveness test

4.2.2.1 Sample preparation

In order to obtain more repeatable data and understand oil dispersion and coalescence more thoroughly, a larger-volume chemical effectiveness test was developed. Artificial seawater (120 ml) was measured with a graduated cylinder and added to 125 ml glass bottles, which were sealed with plastic caps. Using a plastic tipped micropipette, 100 µl of crude oil was added to the surface of the water to reach an oil: water ratio of 1:1200. The dispersant of interest was then applied dropwise to the center of the oil slick using a plastic tipped micropipette for a DOR of 1:50. The oil reacted instantly when dispersant was added. The entire procedure was carried out at a room temperature (about 20 ℃).

4.2.2.2 Sample mixing

After the dispersant was applied to the oil, the glass bottles were attached to a rotating table with an orbital distance of 2 cm and rotating speed of 200 revolutions per minute. The rotational mixing lasted for 30 min, then the bottles were added to 125 ml separatory funnels and

left to stand for 15 min to allow the droplets to stabilize. The separatory funnels were drained sequentially, collecting four 30 ml samples into 45 ml plastic centrifuge tubes.

4.2.2.3 Oil extraction and analysis

Similar to the small-vial tests, in the higher volume effectiveness tests the mass concentration of dispersed oil was determined by extracting the oil into DCM followed by spectrophotometric measurement of the concentration of extracted oil. Ten ml DCM was added to each centrifuge tube (containing its 30 ml sample) and was shaken manually about 30 s to allow the oil and DCM to mix well. The tubes were then left standing a few minutes for DCM/water layer separation. With a repeating pipette, 200 µl of the DCM extraction was added to each well in a 96 well plate followed by spectrophotometer measurements at 340 nm.

4.2.2.4 Experiment Matrix

In this experiment, the effects of polymer size and surface groups were evaluated. All experiments in this set were conducted at the same conditions of pressure and temperature (1 atm and 22 ℃), and the same DOR of 0.02. Triplicate measurements were used to evaluate repeatability. The negative control group, called “oil only”, was the oil added to water without any dispersant or polymer. The following table shows the experimental matrix for higher-volume effectiveness tests.

Table 4-3. Experimental matrix for higher-volume effectiveness tests of various sized hyperbranched polymers and different surface group dendrimers

Experiment number	Polymer	MW (kDa)	Surface group
1	G4-PAMAM-NH2	14	Amino
2	G4-PAMAM-OH	14	Aminoethanol
3	G4-PAMAM-SA	21	Succinamic acid
4	HY-PEI	1.2	Amino
5	HY-PEI	1.8	Amino
6	HY-PEI	10	Amino
7	HY-PEI	70	Amino
8	HY-PEI	750	Amino
9	Corexit	NA*	NA*

*NA = Not applicable

4.2.3 Particle and Droplet Size Distribution Measurement

In order to measure the oil and polymer size distributions we used both a Coulter counter and DLS.

4.2.3.1 Coulter counter

In this experiment, we adopted a hand-held automated cell counter (EMD Millipore) which uses the Coulter principle to measure the particles. We selected a sensor with a 60 μm sample port size, which is appropriate for measuring particle sizes from 6 μm to 36 μm. Oil droplets larger or smaller than this range could not be examined by this instrument.

Thirty three microliters crude oil were added into 40 ml artificial seawater followed by adding either 67 μl of a 1% 10 kDa HY-PEI working solution or a 1% working solution of Corexit. Then the samples were placed on a shaker table and rotated for 30 min. After rotation, 1 ml sample was diluted into 10 ml PBS (phosphate buffered saline) and mixed well. We submerged the sensor into the solutions and the results were reported by the instrument in 30 seconds.

4.2.3.2 Dynamic light scattering

In order to know the drop size distribution in the range of less than 6 μl, we used DLS. Two series of experiments were developed for particle and oil droplet size distribution measurement. One is the hydrodynamic size distribution of hyperbranched polymer itself. Five HY-PEI polymers were dissolved in artificial seawater to reach a mass concentration of one percent, then sonicated for 5 min. One ml of this solution was transferred to a cuvette and measured by Malvern Zetasizer Nano ZS.

The other experiment was to measure the size distribution of dispersed oil drops. Crude oil (33.4 μl) was added to 40 ml artificial seawater in plastic centrifuge tubes and followed by applying the HY-PEI diluted solution (1% mass concentration) to the center of the oil slick reaching a DOR of 0.02. Centrifuge tubes were then placed in a rotating table to shake for 30 minutes at 200 rpm. Immediately after mixing, one ml of the oil/water emulsion sample was placed in cuvettes to measure the oil droplet size distribution. All of the measurements were conducted at 20 ℃.

A Malvern Zetasizer Nano ZS is the instrument we used in these experiments to characterize the particle and oil droplet size distribution. This instrument worked with the mechanism of DLS and it can detect oil drop size ranging from 1 nm to 10 μm. Light from the laser light source illuminates the sample in the cell. The scattered light signal is collected with detectors of 173 degrees (back angle) scattering angle. Particles can be dispersed in a variety of liquids. Only liquid refractive index and viscosity need to be known for interpreting the measurement results. The refractive index used for crude oil was 1.45 and for HY-PEI it was 1.53. Water viscosity around room temperature is 0.001 (Pa·s).

3.2.4 Interfacial Tension Measurement

We used a pendant drop method to measure the interfacial tension between the oil and water interface. We used different methods to test interfacial tension changes in Corexit and dendritic polymers. . For Corexit we used a premix method involving premixing oil and Corexit at a concentration of 500 ppm and putting this premix sample on a shaker table rotating for 24 h. During the experiment, the oil phase was the premix Corexit and oil, and the water phase was artificial seawater. The reason for premixing the oil and Corexit is that the effectiveness of Corexit would decrease dramatically when diluted in water before it was applied to the oil slick (Belore & Ross 2000), and Corexit active ingredients are dissolved in non-polar petroleum distillates. Different from Corexit, hyperbranched polymers are not easily miscible with oil and are dissolved in water from the manufacturer; premixing is thus less effective. In experiment of measuring hyperbranched polymers, the oil phase was crude oil and the water phase was hyperbranched polymers in saline solution. We prepared samples in concentrations of 0.1, 0.05, 0.025, and 0.0125 g/l and all the solutions were prepared immediately before the experiments.

We performed our experiment using a drop shape analyzer called Easy Drop (Kruss, Germany). This instrument mainly consists of a camera with zoom lens, a sample height adjustment table, a 10 x 10 x 10 cm glass cuvette, and a syringe/needle sample delivery unit. Images are recorded via computer and analyzed with the shape analysis software Drop Shape Analysis (DSA) provided by Kruss (Figure 4-2).

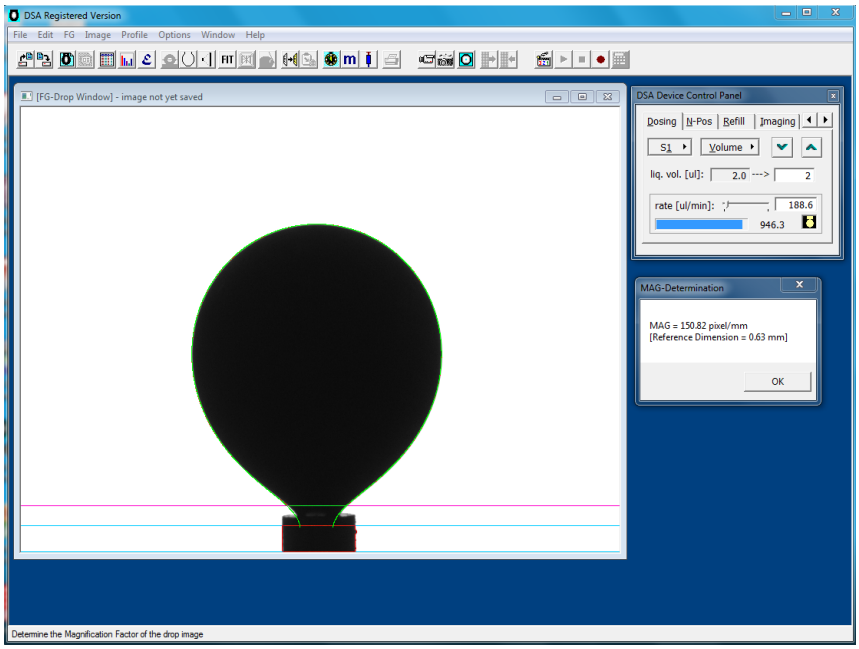

Figure 4-2 Screen shot of drop shape analysis software.

In order to measure oil in water interfacial tension, we selected a floating pendant bubble mode which was performed using a J-shaped needle that delivered oil upward. First the glass cuvette was filled with aqueous solution—either artificial seawater alone or dispersant working solution—and the plastic syringe was loaded with crude oil. Then a 3 µl drop was delivered by the syringe motor controller and a video recording was begun at the same time. In presence of dispersant, the drop shape changed with time as the interfacial tension decreased (Figure 4-3). Eventually (after a few seconds or up to over a minute or two) the interfacial tension was low enough that the drop would be released from the needle.

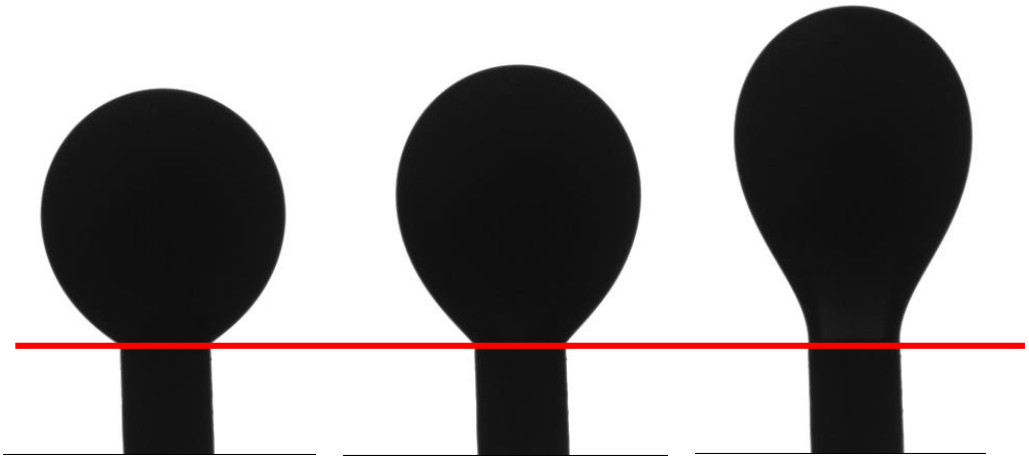

Figure 4-3 Video frames of oil drop shape varied with time. 0.0125 g/L HY-PEI 10kDa at time of 20 s, 70 s and 115 s. Needle diameter is 0.632 mm. As the age of drop increased, the drop shape became elongated.

At steady (or quazi-steady) state, the shape and size of the pendant oil drop are determined by gravity, buoyancy, and surface forces. Buoyancy pulls the drop upwards, increasing elongation. Interfacial tension (which exists at the interface between two immiscible phases) attempts to reduce the contact area by pulling the drop into a spherical shape. The interfacial tension can be determined by characterizing the shape using the Young–Laplace equation.

5 RESULTS AND DISCUSSION

5.1 Preliminary Experimental results

5.1.1 Calibration curve

In order to relate DCM absorbance data with the actual amount of oil dispersed in water, we developed two calibration curves (Figure 5-1). Curve 1 was made by adding oil into artificial seawater and extracting into DCM following the same procedure as used during effectiveness tests. Curve 2 was made by dissolving oil directly into DCM. The linear fit to Curve 1 is in Equation 4-1.

$$y = 3.0399x - 0.0363 \quad (5\text{-}1)$$

Here *y* is the oil concentration in DCM (µl/ml), and x is the absorbance at 340 nm. The R^2 was 0.9967 which shows a good linear fit. The linear fit for Curve 2 is in Equation 4-2.

$$y = 2.4719x + 0.1482 \quad (5\text{-}2)$$

Here again y is the oil concentration in DCM (µl/ml) and x is the absorbance at 340 nm. The R^2 value was again high, 0.9868, showing a good linear relationship. However, by calculating Equation 4-1 and 4-2, we see that the DCM extraction efficiency was not 100% for the higher oil concentrations. Thus, we used Equation 4-1 to calculate the mass of oil in extracted samples, based on the absorbance measurements.

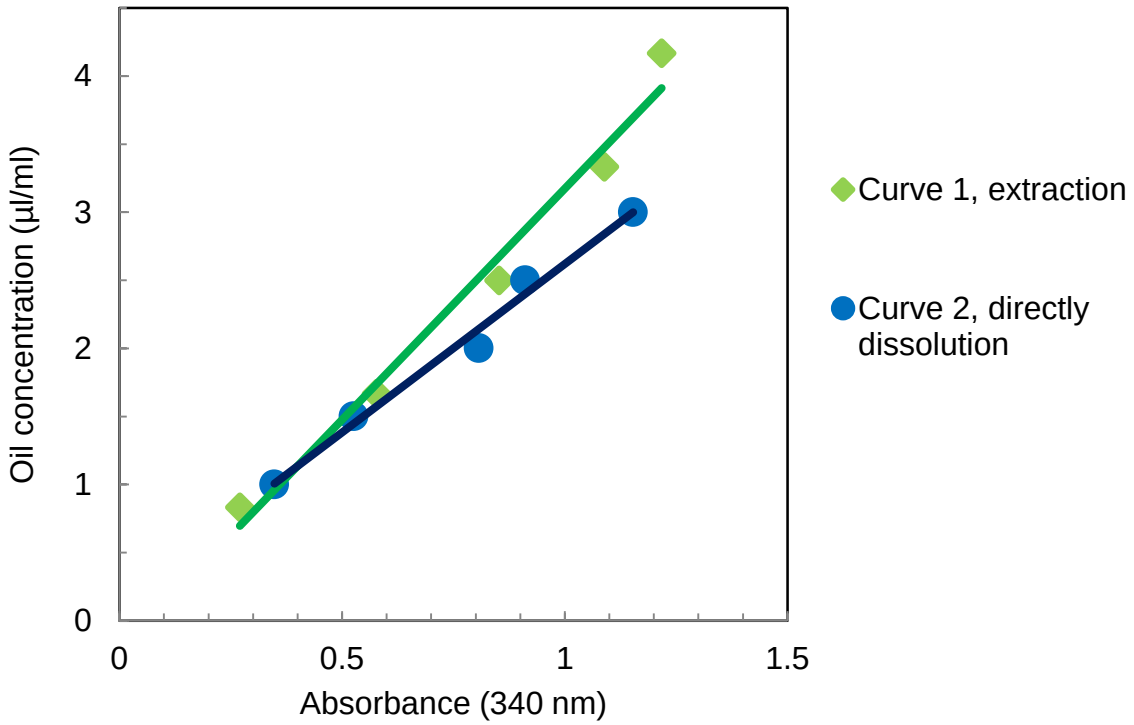

Figure 5-1 Calibration curves of oil extraction method and oil dissolution method.

5.1.2 Small vials trial

In initial experiments using the small vials protocol, two dendritic polymers, 10 kDa HY-PEI and G4-PAMAM-NH_2 were tested for their dispersion effectiveness under three different DORs. These were compared with commercial dispersant Corexit 9500. Figure 5-2 shows the data, with the y-axis being the amount of oil dispersed in the water column divided by the total amount of oil added to the sample; thus the number should be less than or equal to 1. When no dispersant was added, there was a limited amount of oil dispersed in the water; even though the oil/water emulsion is unstable, some of the oil was entrained in the water column. After a period of settling, the oil drops in both dispersed and non-dispersed samples coalesced and floated up to the water surface. The dispersant addition caused this time to increase greatly. At a DOR of 0.02

the effectiveness of Corexit and HY-PEI were about 0.55 and 0.71. The effectiveness of G4-PAMAM-NH_2 increased to 0.27 which is much larger than the 0.02 found when no dispersant was added. When increasing the DOR, there is an increasing trend of oil dispersed in the water for the polymers, with effectiveness of HY-PEI and G4 reaching 0.93 and 0.67 at a DOR of 0.08. However, the effectiveness of Corexit decreased with increasing DOR, which was counter to our expectation.

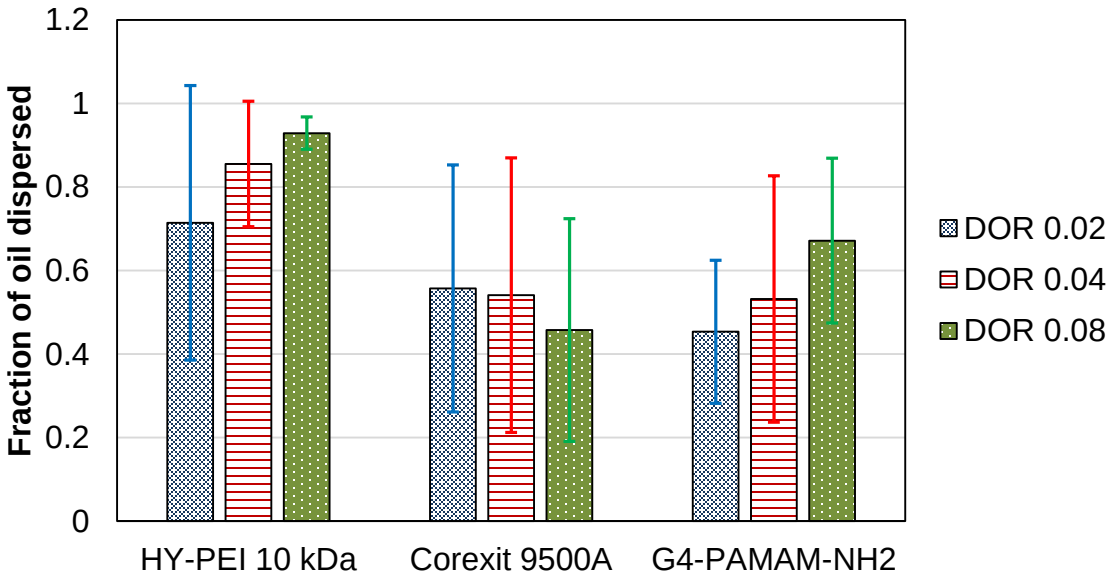

Figure 5-2 Fraction of oil dispersed by three materials at three dispersant to oil ratios in the first small-vial experiment. These tests were done without premixing the oil and dispersant, and used the top-insertion sample collection method. Error bars show standard deviation of six samples.

Mixing and settling effects were evaluated in a separate experiment. In order to figure out the appropriate mixing and settling time we choose three combinations (mixing / settling) 24 hr / 2 hr, 1 hr / 30 min, and 30 min / 15 min. The results are shown in Figure 5-3. The highest effectiveness, 0.83, appeared with the 30 min / 15 min case. The effectiveness at 1 hr / 30 min and 24 hr / 2 hr were 0.64 and 0.66, seems smaller than the 30 min / 15 min case. In a previous study longer mixing times led to higher effectiveness because more energy is applied to break oil into droplets and better contact is achieved between dispersant and oil. Longer settling times

resulted in low effectiveness because of coalescence and floating of the oil (Sorial *et al.* 2004*a*). In our tests it was apparent that settling time was most important, so for future experiments we chose the shortest settling time (15 min). We also chose the shortest mixing time (30 min) for convenience, since even the shortest mixing time provided sufficient energy and contact to show good dispersion.

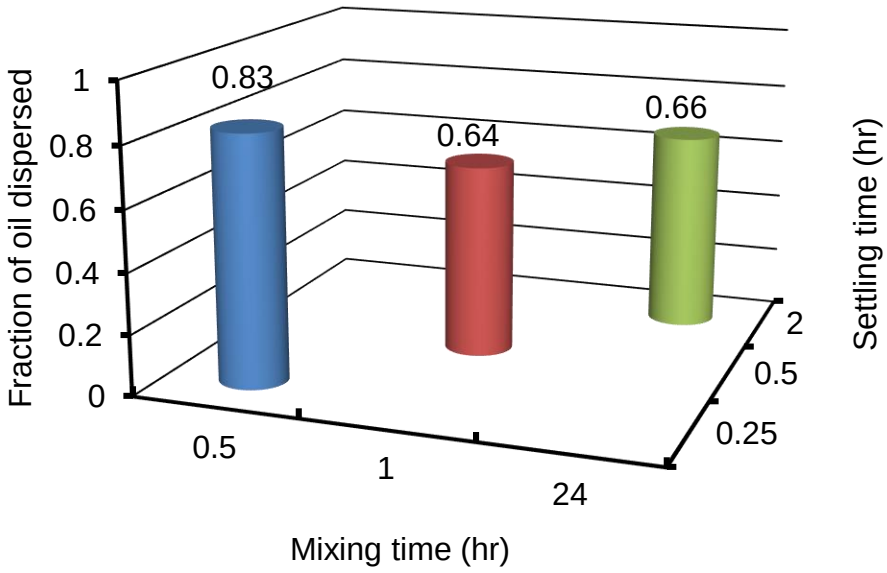

Figure 5-3 Fraction of oil dispersed by 10 kDa HY-PEI at different mixing and settling times. These tests were done without premixing the oil and dispersant, and used the top-insertion sample collection method.

Figure 5-4 shows the results of different sample preparation and collection methods. Two sample preparation methods, premix and non-premix and two sample collection methods, side penetration and top insertion. The results did not show clear trends as to how these different sample preparation and collection methods influenced the effectiveness. The methods gave different results about which polymer had better dispersion ability, though there was an overall result of the three high molecular weight polymers having better dispersion capability than the two low molecular weight polymers. Also, replicate experimental results (not shown) were quite different with one other. It was hypothesized that the small sample volume made the results

unrepeatable, leading to our development of the higher volume effectiveness protocol (data shown later).

It was also observed that the premix method often used in the oil dispersion literature was not applicable for hyperbranched polymers. In the premix method, we first mixed the crude oil with polymer working solution which contained 99% water. Since water and crude oil are immiscible, the oil-polymer premix was not homogenous and polymer concentration likely varied in each separate drop removed from the premix vial. The premix method did work for Corexit, as the active ingredients (surfactants) are dissolved in an oil-miscible petroleum distillate solvent.

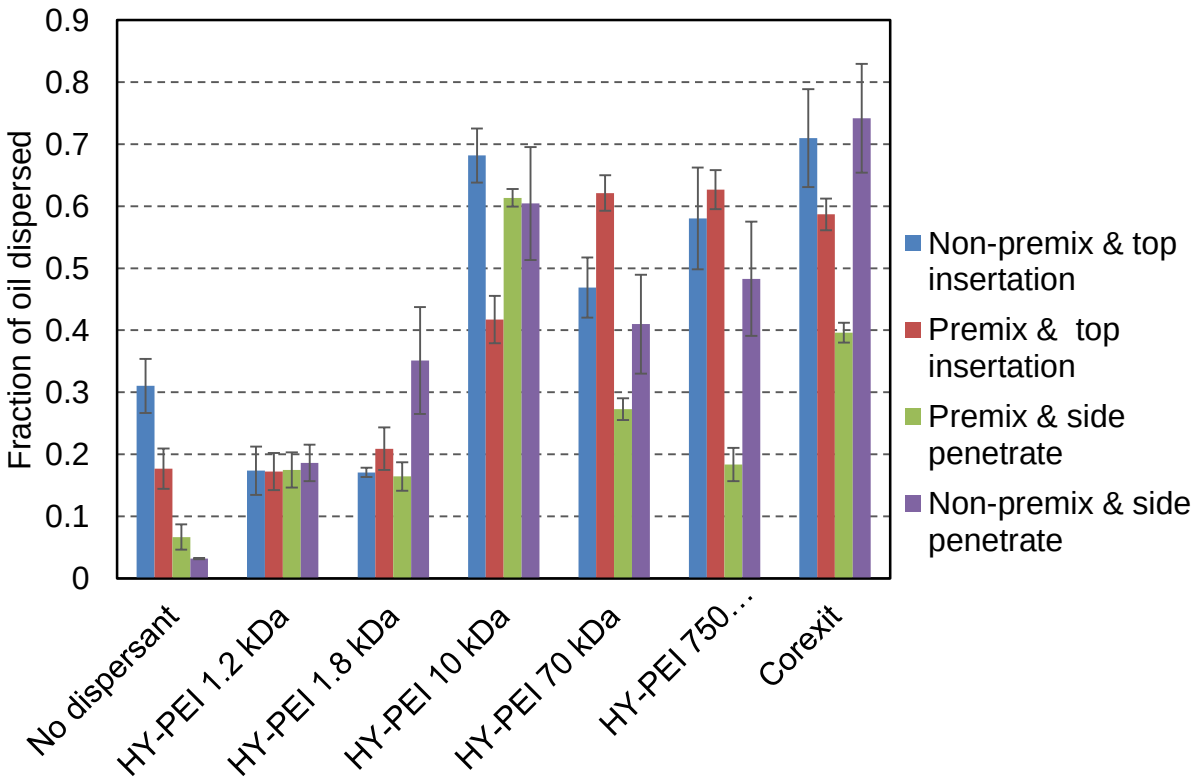

Figure 5-4 Effectiveness results of various sample preparation and collection methods.

5.2 Higher-volume chemical effectiveness results

5.2.1 Effect of molecular weight on dispersion effectiveness

The effects of various molecular weights on dispersion capacity of dendritic polymers were tested using the higher-volume protocol, including a separatory funnel. Data are shown in Figure 5-5 and Figure 5-6. The five HY-PEI polymers were used, with the same chemical structure but different molecular weight ranging from 1.2 kDa to 750 kDa. The dispersion ability was compared with commercial dispersant Corexit and no dispersant (oil only) scenarios. Each sample preparation resulted in four data points representing the 30 ml column segments of water from the bottom to top of the separatory funnel. Figure 5-5 shows the fraction of oil dispersed in each of these four column segments. Figure 5-6 shows the total dispersion effectiveness of the overall sample, which we defined as the sum of the fractions of oil dispersed in the bottom three segments (90 ml of the 120 ml total sample volume). This leaves out the top segment, which could contain non-dispersed oil floating on top of the sample.

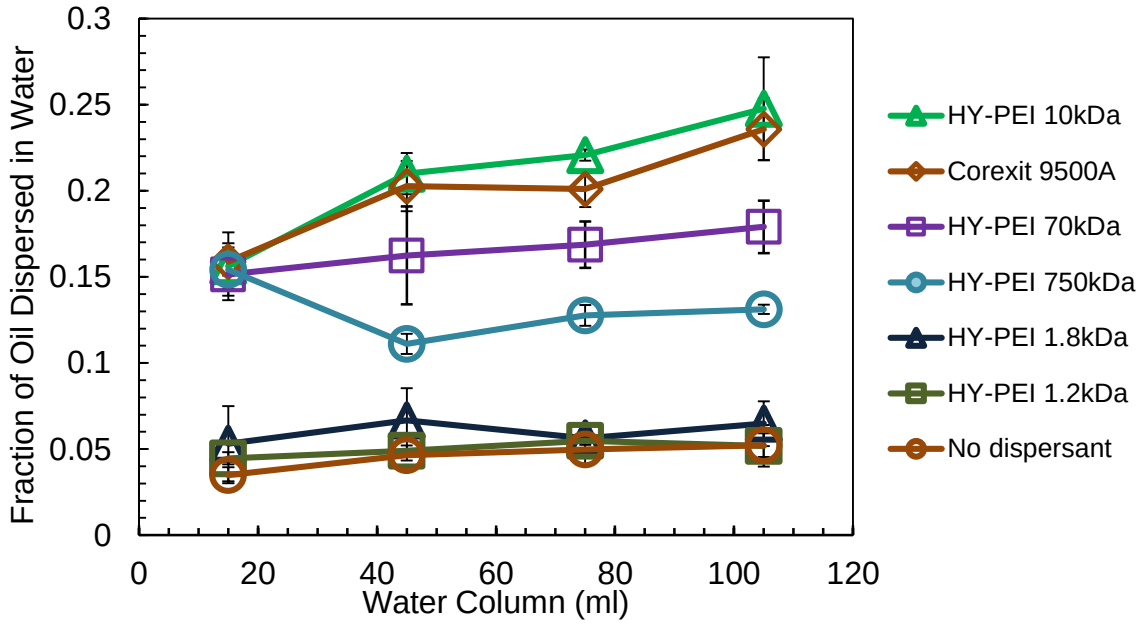

Figure 5-5 Fraction of oil dispersed by HY-PEI in each 30 ml increment of the water column.

HY-PEI 10 kDa, 70 kDa, 750 kDa and Corexit dispersed more oil in all four water column segments than HY-PEI 1.2 kDa and 1.8 kDa. Compared with the no dispersant scenario, HY-PEI 1.2 kDa and 1.8 kDa seemed to have little dispersion ability; HY-PEI 1.2 kDa dispersed 11% crude oil in first three water column segments which is smaller than the 13% oil dispersed with no dispersant, and HY-PEI 1.8 kDa dispersed 18%. HY-PEI 10 kDa, 70 kDa, and Corexit showed the expected tendency that the mass of oil dispersed increases with the height of water column. Oil and water are two immiscible liquids and these oil-water emulsions were unstable; or at least some of the droplets were unstable and rose in the column. After mixing by shaking 30 min, the oil mass distribution should have been identical in each water column segment, but during the 15 min settling period when no shear force was introduced, small oil droplets flocculated and coalesced, resulting in larger oil drop formation. The large oil drops resurfaced due to buoyant forces which increased with the size of the oil drop.

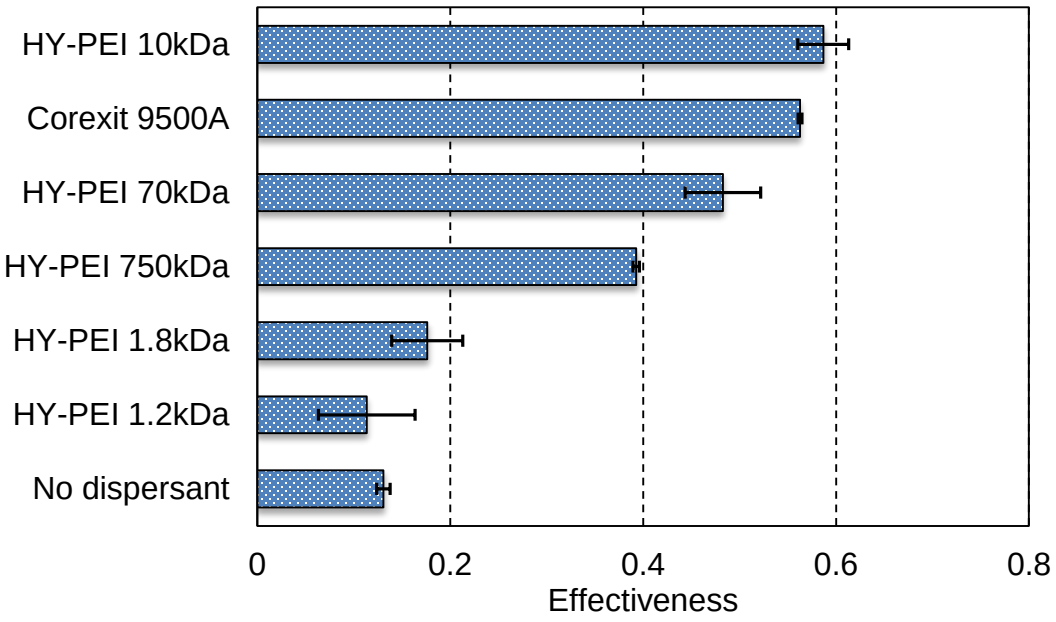

Figure 5-6 Effects of molecular weight on dispersion effectiveness of HY-PEI.

Contrary to the above explanation and results seen with Corexit and most polymers, the HY-PEI 750 kDa sample had more oil remain in the bottom column segment. Sixteen percent of oil dispersed in that lowest segment while only 10% and 12% oil dispersed in second and third. One explanation could be that the oil-polymer complexes were actually denser enough to sink. Similar phenomenon has been observed in natural systems that application of chemical dispersants in coastal waters may increase oil sedimentation due to oil-SPM (suspended particulate matter) aggregation (Khelifa *et al.* 2006). And this oil-SPM will finally settle down to the bottom of sea unless it is biodegraded during the sedimentation. And the anaerobic conditions in sea bottom is an obstructor for oil biodegradation by microorganism.

In Figure 5-7 we plotted the data in another way to show the relationship between the molecular weight of polymer and its effectiveness. The X-axis is the molecular weight of five hyperbranched polymers and the y-axis is the fraction of oil dispersed in each column. HY-PEI 10 kDa shows the highest performance of dispersing the oil, followed by HY-PEI 70 kDa and 750 kDa. HY-PEI 1.2 kDa and 1.8 kDa showed less capacity of dispersion. A previous study by our collaborators showed that oil molecules incorporated into the hyperbranched polymers (Geitner *et al.* 2012). So we hypothesize that hyperbranched polymers with a large molecular weight may have a larger interior space which can hold more oil molecules. In contrast, small polymers with less interior space may have less hosting capacity. However, the effectiveness decreased when molecular weight was over 10 kDa. This may result from the fewer number of large polymers existing in the mixture. Since we added the polymer by equal mass, the polymer with large molecular weight has a lower molar concentration. The total interior space created by large polymers such as HY-PEI 70 kDa and 750 kDa was likely actually smaller than the total

interior space created by HY-PEI 10 kDa; this manifested itself as lower effectiveness in oil dispersion.

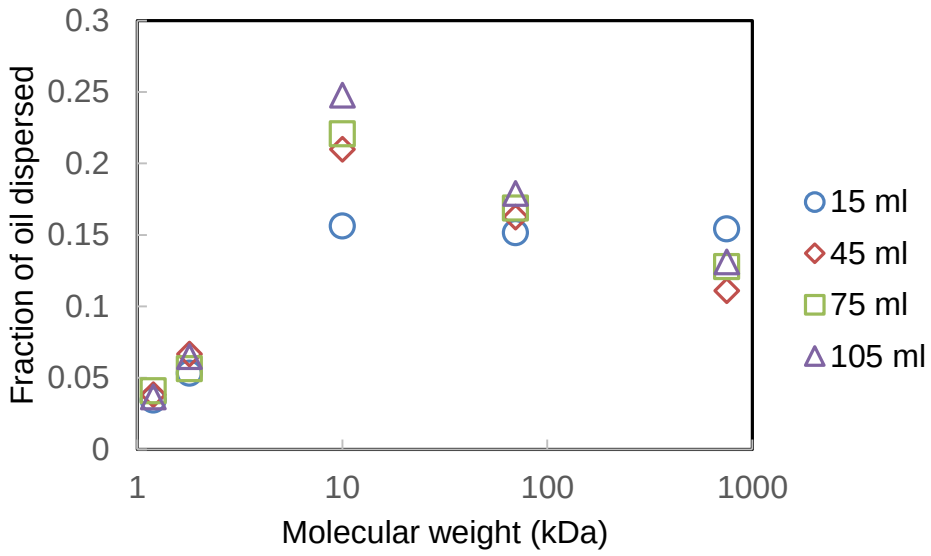

Figure 5-7 Relationship between molecular weight and fraction oil dispersed by each water column

Further examining the data, Figure 5-8 shows the relationship between the polymer molecular weight and the oil incorporation capacity for single polymer molecule. In order to calculate how many oil molecules were dispersed by a single polymer molecule, we made several assumptions. Our first assumption was about the average molecular weight of crude oil. Mass spectrum of crude oil showed the mean value is about 500 g/mol (Magnet lab 2014). We only calculated the oil dispersed in the first three water column segments and assumed that only 1.5 µl polymer was incorporated with the oil. The molecule number was obtained by dividing the mass by the molecular weight therefore we can get the oil/polymer molecule number ratio.

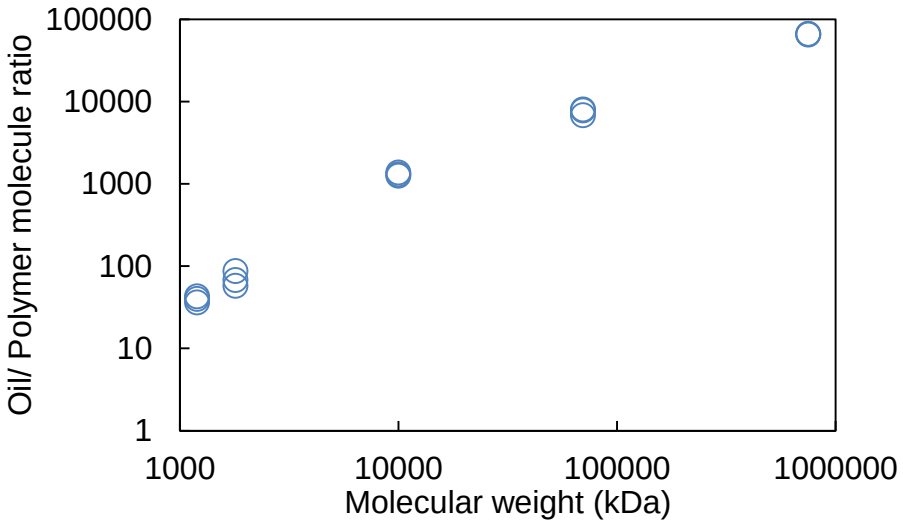

Figure 5-8 Molecular ratio of oil to polymer in dispersed system.

From Figure 5-8, we can observe that the oil/polymer molecular ratio increased with the molecular weight of the polymer which indicates that the large polymers can entrap more oil molecules than smaller polymers, which was expected. The magnitude of the ratio ranged from 50 to 100,000. For example, with HY-PEI 10 kDa, one polymer molecule can incorporate 1,000 oil molecules. However, the molecular weight of HY-PEI 10 kDa is only 20 times larger than the oil molecule. This indicates that the way the polymer interacts with oil is not limited to encapsulation because one polymer cannot hold 1,000 oil molecules. So we hypothesized a new mechanism where the polymer may have surfactant-like characteristics where polymers coat the surface of oil droplets and lower their interfacial tension. Alternatively, the globular structure of the polymers may share some properties with particles such as carbon black which stabilize oil through a Pickering emulsion mechanism.

5.2.2 Effects of polymer end group on dispersion effectiveness

The effect of different surface groups on dispersed oil is shown in Figure 5-9. The three dendrimers have the same interior structure, similar molecular weight but different outer

functional groups. The amino group in G4-PAMAM-NH_2 had a positive surface charge, amidoethanol group in G4-PAMAM-OH is neutral and succinamic acid groups in G4-PAMAM-SA are negative. G4-PAMAM-NH_2 had a certain capability to disperse oil, though it was weaker than Corexit. Dendritic polymers with neutral and negative charge showed barely any potential for oil dispersion. This may result from the electrostatic force between the polymers and oil drops. Typically oil drops acquire a certain number of negative charges in aqueous solution, so they would attract polymers with a positive surface charge and repel polymers with negative charge. As for neutral surface charge, there would be only a weak interaction between the polymers and the oil drops. Therefore neutral and negatively charged polymers can hardly adsorb on the oil drop which results in low effectiveness.

This also points to another mechanism of stabilization for dendritic polymers with positive charge. They may form a surface coating making the particles have an overall positive

charge, and an electrical double layer. This double layer gives electrostatic repulsion between the oil drops and keeps them away from each other therefore stabilizing the oil-water emulsion.

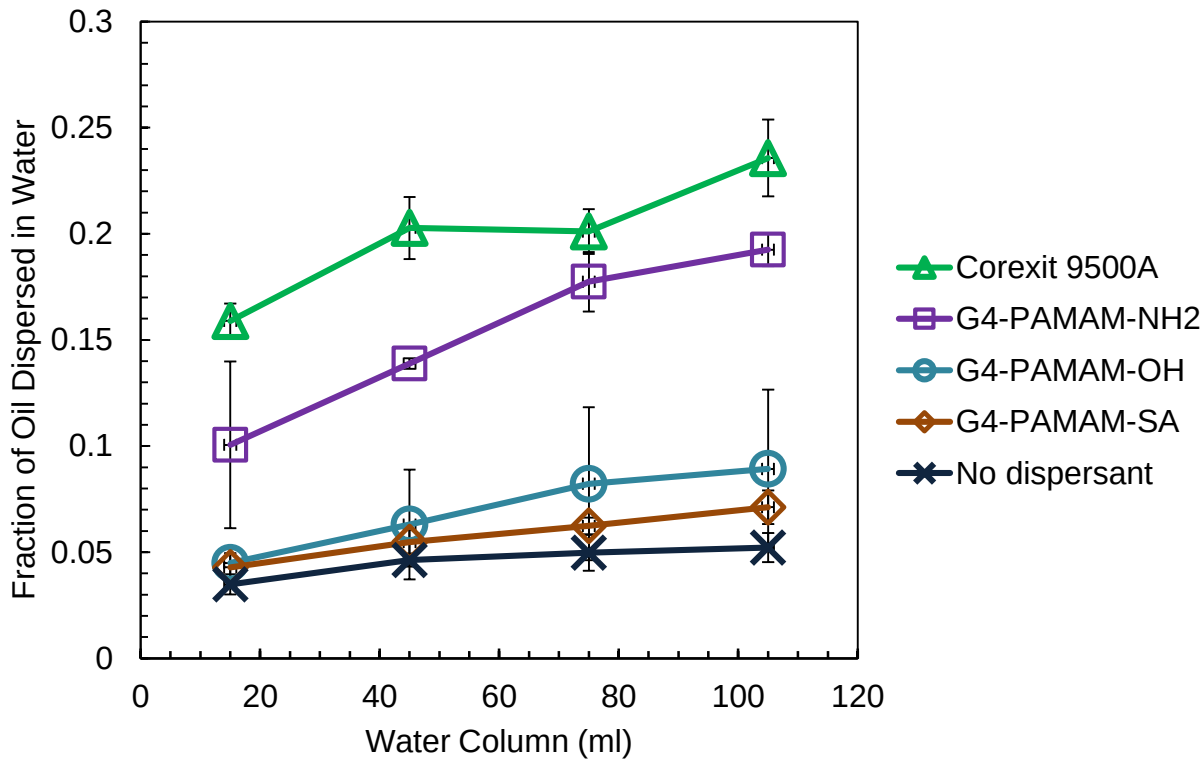

Figure 5-9 Effectiveness of dendritic polymer with different surface functional groups.

5.3 Particle and oil droplet size distribution results

5.3.1 Coulter counter results of oil drop size distribution

Figure 5-10 shows the droplet size distribution of oil dispersed by HY-PEI 10 kDa and Corexit. It should be stressed that the Coulter counter particle size results were not repeatable with this instrument. On a different day an attempt was made to measure particle sizes for all of the polymers, but the instrument would not function well enough to produce data. Thus these results should be treated with caution; they are presented here as evidence to indicate particle

size, but they are not conclusive. Since the instrument can only present the drop size range from 6 µm to 36 µm, the oil drop size besides this range is not shown in Figure 5-10. It is probably that the oil drops in Corexit sample tended to have smaller droplet size than HY-PEI 10 kDa. And oil drop size distribution in both samples mainly lay in the range less than 7 µm. This result indicates that we should examine the oil droplet smaller than 7 µm to get a better understanding of drop size distribution behavior. In Corexit, 58 percent of the oil droplets were smaller than 6 µm and the largest drop size was 8.4 µm. However, only 28 percent of the oil drops in HY-PEI sample were smaller than 6 µm and the largest drop size was 9.4 µm. We can conclude that the large numbers of oil drops were smaller than 6 µm in both samples. Corexit formed more small oil drops than HY-PEI 10 kDa.

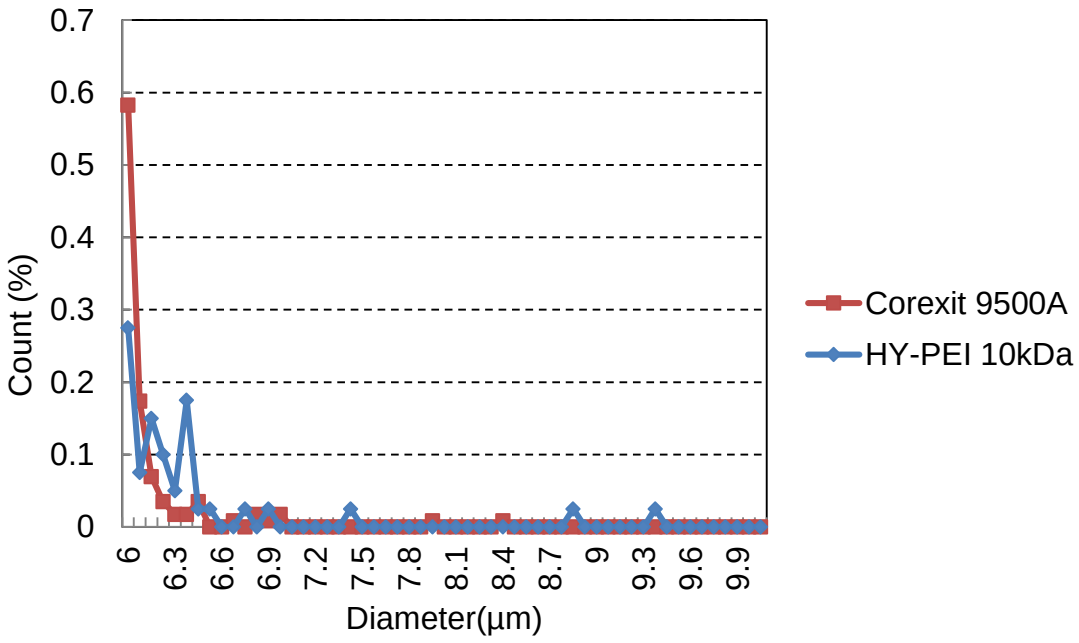

Figure 5-10 Normalized result of drop size distribution of crude oil dispersed by HY-PEI 10 kDa and Corexit.

5.3.2 DLS results of hydrodynamic size of hyperbranched polymers

Table 5-1 shows the hydrodynamic size of hyperbranched polymers with different molecular weight. The molecular weight increased as hydrodynamic size increased. The smallest HY-PEI 1.2 kDa polymer had a size of 2 nm and the largest HY-PEI 750 kDa had a size of 32 nm. HY-PEI 10 kDa had a diameter of 6 nm which is consistent with previous data (Geitner *et al.* 2012).

Table 5-1 hydrodynamic size of hyperbranched polymers.

Polymer	HY-PEI	HY-PEI	HY-PEI	HY-PEI	HY-PEI
MW (kDa)	1.2	1.8	10	70	750
Hydrodynamic size (nm)	2.00	2.05	6.09	10.96	32.03

5.3.3 DLS results of hydrodynamic sizes distribution of oil droplets dispersed by hyperbranched polymer

Figure 5-11 shows the volume distribution of dispersed oil by hyperbranched polymers and Corexit. The volume distribution refers to the total volume of oil within the droplets of a certain size. Since the oil droplets were measured by DLS, the droplets smaller than 1 nm and larger than 10 μm were not detected by the instrument. Oil dispersed by 10 kDa HY-PEI had a mean size of 1990 nm, slightly smaller than that of Corexit, 2300 nm. One group examined the volume distribution for Arabian light crude oil and found that the mean size of oil drops dispersed by Corexit was around 3500 nm (Mukherjee & Wrenn 2011), on the same order of magnitude with our measurements, though larger. Oil droplet size distribution patterns of HY-PEI 70 kDa and 750 kDa were similar and the mean size was larger than HY-PEI 10 kDa. Oil dispersed by HY-PEI 1.8 kDa had the largest mean size of 5559 nm and the oil distribution in 1.2 kDa HY-PEI cannot obtain by DLS data; it may be too large and unstable to be detected by the

instrument. Previously it was shown that the smaller the size distribution the better the dispersion performance (Mukherjee & Wrenn 2011). Our results were difficult to repeat and the data are inconclusive as to the actual size of droplets obtained in our work; however, the data available are consistent with the hypothesis that the dispersed oil droplets are much larger than the polymers, which means that the main mechanism of dispersion may not be encapsulation into the polymers, but surfactant-like or Pickering emulsion instead. Aggregation of polymers with encapsulated hydrocarbons is also a possibility.

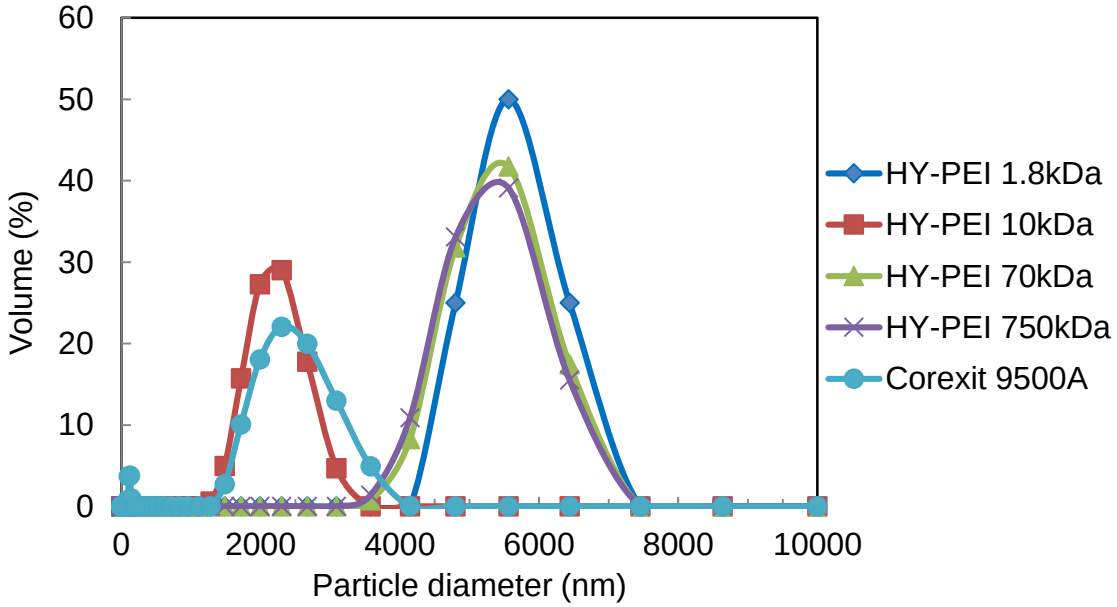

Figure 5-11 Volume distributions for dispersed oil.

5.3.4 Conceptual model of oil drop size distribution

As mentioned previously, it is assumed that after shaking for 30 min the oil drops were equally distributed in the water column of the separatory funnel. During the subsequent 15-minute settling period the drops coalesced and rose. In order to check our theoretical understanding of the system regarding oil droplet size we built a conceptual model using the Stokes terminal settling (rise) velocity equation (Equation 4-3). By calculating the terminal

velocity we could determine the theoretical maximum size of the oil drops in the four water column segments.

$$\mathrm{Vt} = \frac{g d^2 (\rho s - \rho)}{18 \mu} \qquad (5\text{-}3)$$

In equation 4-3 Vt is the terminal velocity of the oil drop floating up to the water surface, g is the acceleration of gravity, μ is the water viscosity, ps-p is the density difference between the water and crude oil, and d is the diameter of the oil drop.

We measured the heights of each of the four water column segments in the separatory funnel and calculated the rise velocities by dividing the height by the settling time of 15 min. We estimated the largest possible oil drop in each water columns (Figure 5-12). The largest oil droplet size in the first 30 ml water column (from bottom to top) was 29 μm which was larger than the 7.5 μm in the sample of HY-PEI 1.8 kDa measured by DLS and 9.4 μm of HY-PEI 10 kDa measured by the Coulter counter. We can conclude that the testing results of DLS and Coulter counter are in the range of the theoretical size of the largest possible oil drop which indicates that the results are consistent with theory. Further, these results suggest that the maximum droplet sizes that could have been formed by the polymer-oil dispersions in our effectiveness tests were 29, 33, 35, and 37 μm for the four respective water column segments.

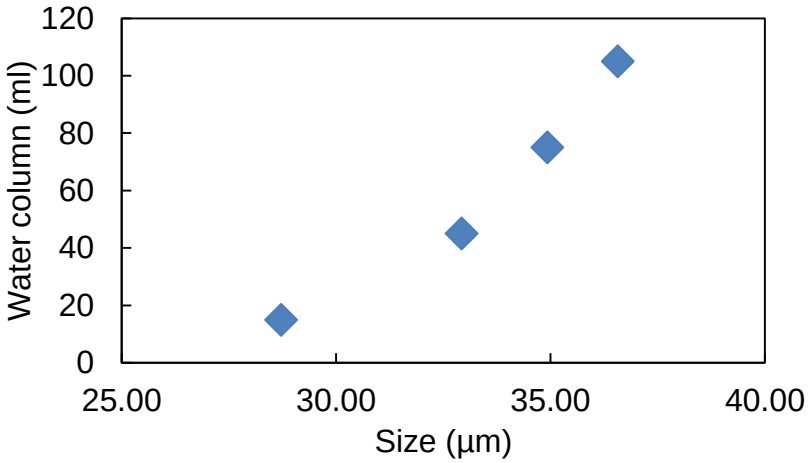

Figure 5-12 Conceptual size of largest oil drops in each water column.

5.4 Oil /water interfacial tension measurement

In interfacial tension experiments, we measured the dynamic interfacial tension in the oil –dispersant–water system by making a series of HY-PEIs and Corexit artificial seawater solutions with different concentrations. By taking videos, the drop shape and interfacial tension were recorded and analyzed.

Figure 5-13 shows the dynamic interfacial tension in a Corexit sample and no dispersant sample. Corexit was premixed with the crude oil for 24 hr with a concentration of 500 ppm (dispersant in oil). A 3 µl oil drop was delivered from the tip of the needle and the video recording was started at the same time. Right after a stable drop formed, the interfacial tension between oil and water was 10.7 mN/m. This number rapidly decreased to 3.79 mN/m at drop age of 40 seconds when the interfacial tension was too small to hold the drop against buoyancy forces and the drop floated away; this is the drop release point. In no dispersant sample, interfacial tension started with a value of 18 mN/m, and then reached a consistent number around 12 mN/m.

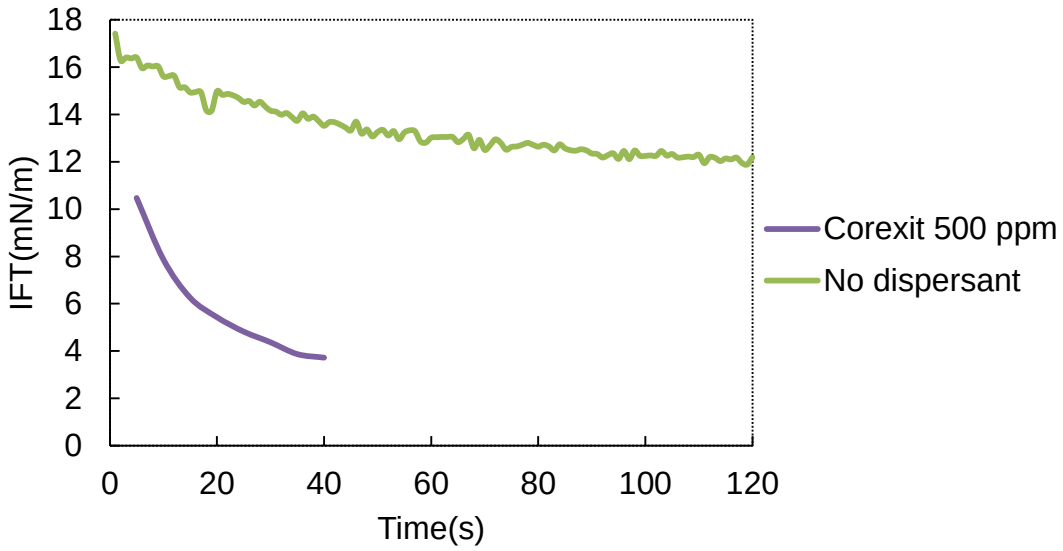

Figure 5-13 Dynamic interfacial tension of curve of Corexit pre-mixed with oil at a concentration of 500 ppm.

Figure 5-14 to Figure 5-18 show the dynamic interfacial tension of 5 HY-PEIs in four different concentrations, 0.0125 g/L, 0.025 g/L, 0.05 g/L and 0.1 g/L. Here the concentrations refer to the polymer dissolved in the artificial seawater phase. By changing the polymer concentration in water phase we examined the effect of dispersant concentration on interfacial tension.

Figure 5-14 shows the dynamic interfacial tension of 1.2 kDa HY-PEI at four different concentrations. All four curves show the same trend that interfacial tension declined with the increasing age of drops. The interfacial tension started with values of 15, 13.25, 10.63 and 5.8 mN/m and end up with 10.79, 9.15, 7.25 and 3.5 mN/m at concentrations of 0.0125, 0.025, 0.05, 0.1 g/L, respectively. The higher the concentration of polymer the lower the interfacial tension. At concentration of 0.1 g/L the interfacial tension decreased to 3.5 mN/m at age of 20 s reaching the drop release point.

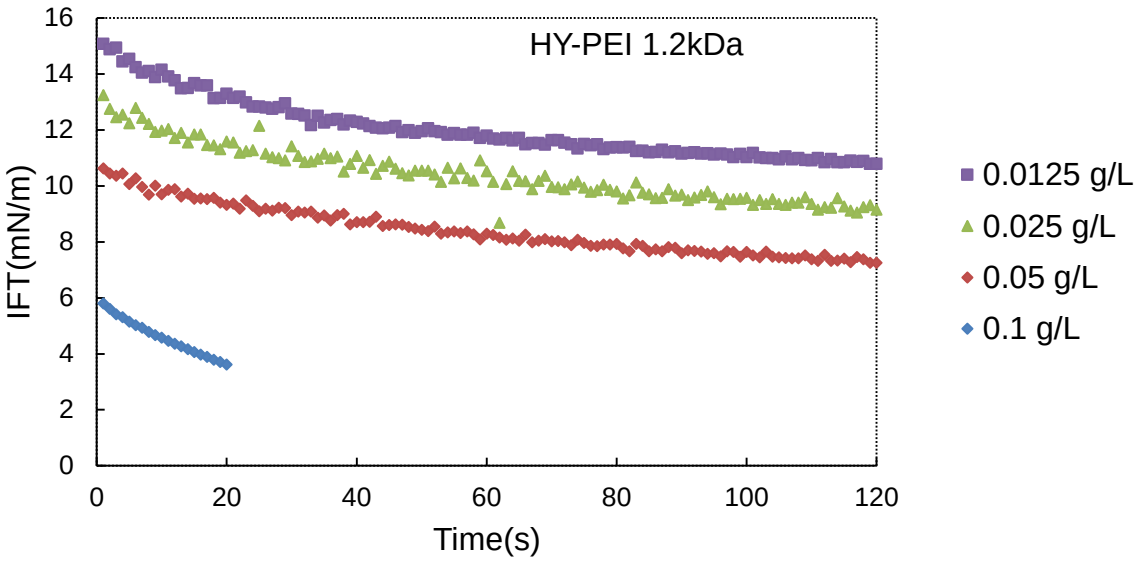

Figure 5-14 Dynamic interfacial tension curve of HY-PEI 1.2 kDa at concentrations of 0.0125 g/L, 0.025 g/L, 0.05 g/L and 0.1 g/L of polymer dissolved in artificial sewater.

Figure 5-15 shows the dynamic interfacial tension of 1.8 kDa HY-PEI at three different concentrations. The interfacial tension at three curves started with values of 16, 12, and 10 mN/m at concentrations of 0.0125 g/L, 0.025 g/L and 0.05 g/L. After 2 min the interfacial tension in the three concentrations seemed to reach a stable value around 6.8 mN/m.

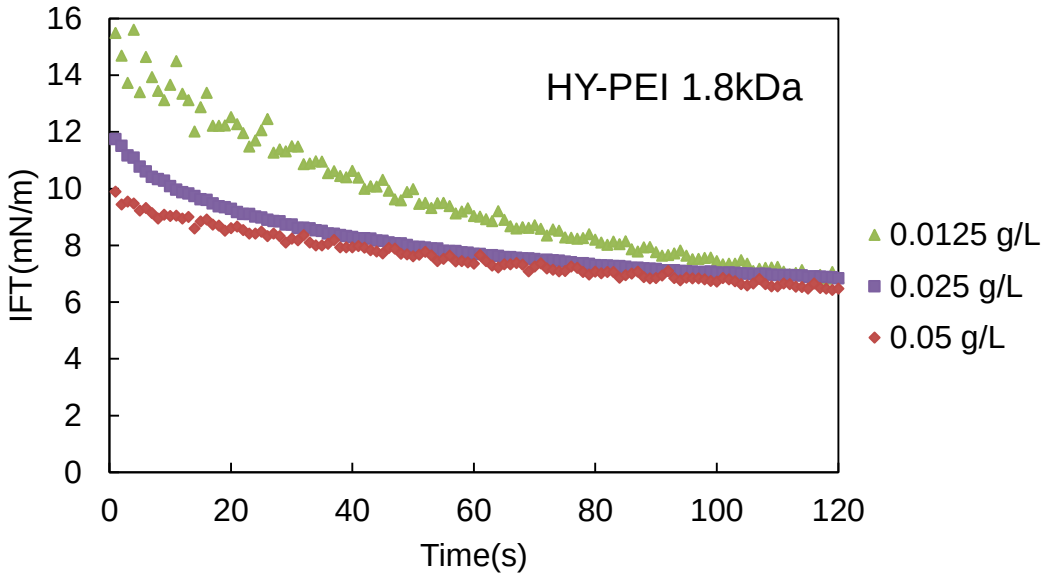

Figure 5-15 Three dynamic interfacial tension curve of HY-PEI 1.8kDa at concentration of 0.0125 g/L, 0.025 g/L and 0.05 g/L

Figure 5-16 shows the dynamic interfacial tension of 10 kDa HY-PEI at different concentrations. All four curves show a similar pattern that interfacial tension declined with increasing drop age. At the same drop age, the interfacial tension is smaller with higher polymer concentration. For example, at the time when the stable drop just formed, interfacial tension started with a values of 15, 12, 7, 5.2 mN/m at concentrations of 0.0125 g/L, 0.025 g/L, 0.05 g/L and 0.1 g/L, respectively. Only at a concentration of 0.0125 g/L did the drop last for 2 min. At the other three concentrations the drop release point occurred before 2 min since the interfacial tension dropped down around 3.5 mN/m.

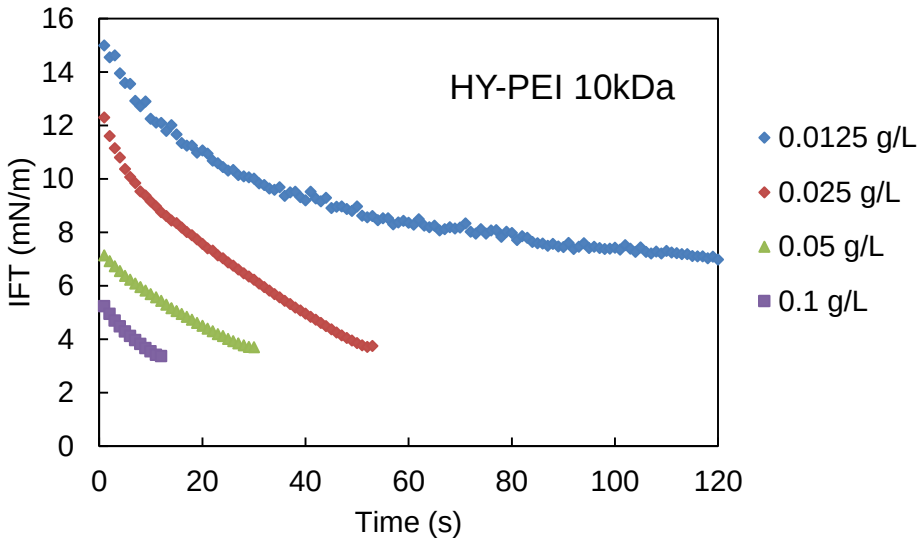

Figure 5-16 Dynamic interfacial tension curves of HY-PEI 10kDa at concentration of 0.0125 g/L, 0.025 g/L, 0.05 g/L and 0.1 g/L.

Figure 5-17 shows the dynamic interfacial tension curve of 70 kDa HY-PEI at different concentrations. All four curves had the trend that interfacial tension decreased with drop age which is similar with 10 kDa HY-PEI. However, the 70 kDa had a stronger reduction effect on interfacial tension than 10 kDa HY-PEI at the same concentrations. For example at a concentration of 0.05 g/L and 0.1 g/L, the interfacial tension in 70 kDa started at 8, and 6 mN/m respectively and reduced to 3.5 mN/m at the age of 12 s and 4 s, respectively. Compared to the dynamic interfacial tension in 10 kDa HY-PEI, the interfacial tension started with 7 and 5.7 mN/m at concentrations of 0.05 g/L and 0.1 g/L, and then dropped down to 3.5 mN/m at age of 30 s and 10 s, respectively.

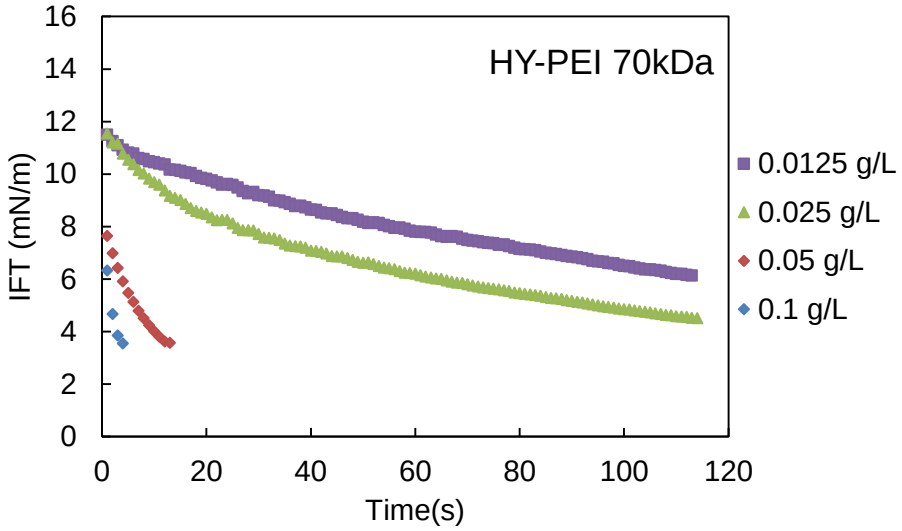

Figure 5-17 Dynamic interfacial tension curves of HY-PEI 70 kDa at concentration of 0.0125 g/L, 0.025 g/L, 0.05 g/L and 0.1 g/L.

Figure 5-18 shows the dynamic interfacial tension curve of HY-PEI 750 kDa at three concentrations. At 0.0125 g/L and 0.025 g/L, the interfacial tension dropped from 12 mN/m to 5.94 mN/m and 4.51 mN/m respectively, reaching the drop release point. When concentration reached to 0.05 g/L, the drop stayed at the top of the needle for only 8 seconds with the final surface tension of 3.8 mN/m.

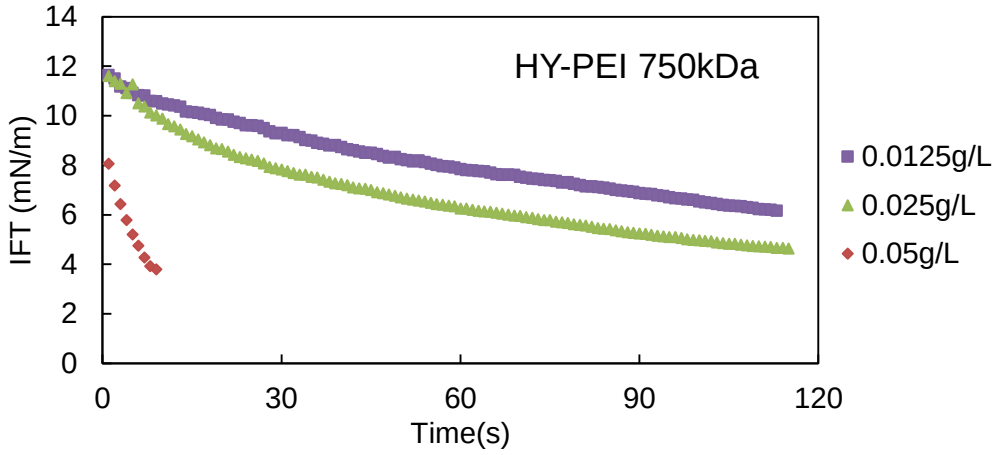

Figure 5-18 Three dynamic interfacial tension curve of HY-PEI 750 kDa at concentration of 0.0125 g/L, 0.025 g/L and 0.05 g/L.

In Figure 5-14 to Figure 5-18, the oil water interfacial tension decreased as the drop aged. This is perhaps because the polymer molecules have an amphiphilic structure with a hydrophilic surface and a hydrophobic interior. HY-PEI has a tendency to stay at the oil/water interface therefore the discrete polymer molecules in bulk water moved to the oil drop surface and adsorbed onto it while reducing the oil/water interfacial tension like a surfactant. In the control group with no dispersant added, the interfacial tension stayed at 12 mN/m after a short aging period. All five hyperbranched polymers were able to reduce the interfacial tension and as the concentration increased the interfacial tension dropped more dramatically.

Figure 5-19 shows the final interfacial tension for five HY-PEI sizes at three concentrations. We did not put the interfacial tension of Corexit here since Corexit sample is prepared in premix method and have a much small concentration. At 0.025 g/L and 0.05 g/L, interfacial tension in HY-PEI 10 kDa, 70 kDa and 750 kDa dropped to around 3.5 mN/m, which is a typical value at the drop release point, while interfacial tension in HY-PEI 1.2 kDa and 1.8 kDa remained around 7.8 mN/m. We can conclude that hyperbranched polymers with high molecular weight, 10 kDa, 70 kDa and 750 kDa have better ability to reduce the interfacial tension than smaller molecular weight polymers 1.2 kDa and 1.8 kDa, and as the concentration increased, all polymers showed greater capacity to decrease the interfacial tension. Compared the interfacial tension data with chemical effectiveness data, we found that even though the Corexit working best in reducing the interfacial tensioin, the chemical effectiveness is similar with HY-PEI 10 kDa and 70 kDa. This may because the polymer is not a surfactant and its working mechainsim is different with Corexit. Surfactant is very effective when reach the critical micelle concentration. However, as for Pickering emulsion, even though in the low concentration, particle can still formed stable emulsion.

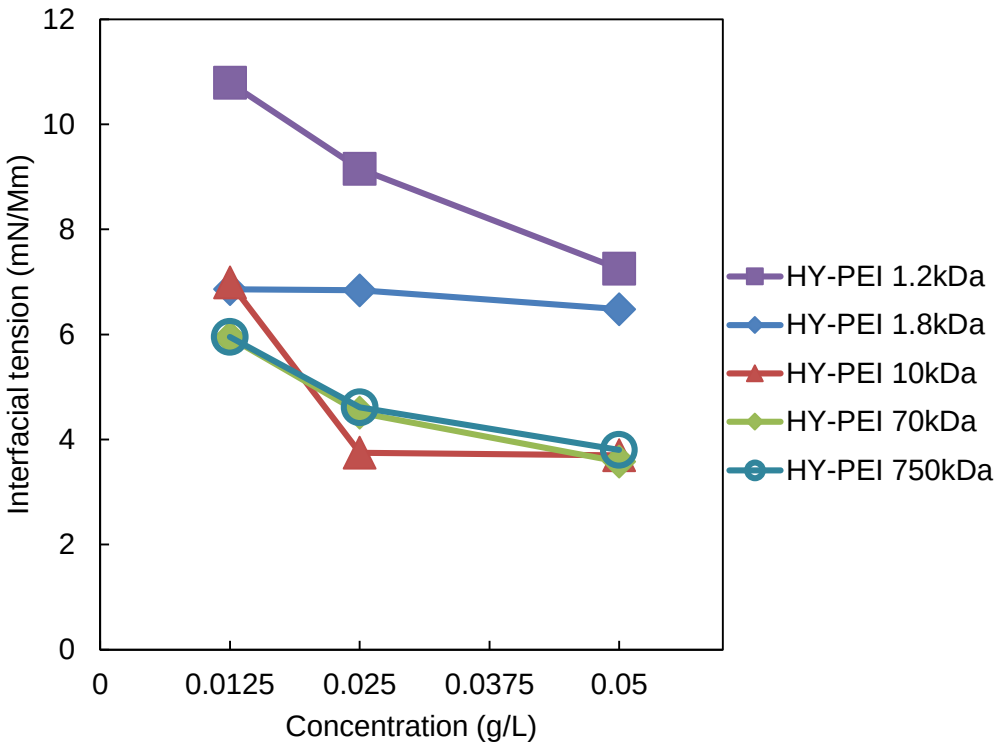

Figure 5-19 Final interfacial tensions for hyperbranched polymers under different concentrations.

6 CONCLUSIONS AND RECOMMENDATIONS

6.1 Conclusions

The first conclusion from this work relates to method development. Using only 12 ml water volume in 20 ml scintillation vials (our "small-volume" trials) resulted in significant variability in dispersion effectiveness data. Using 120 ml water volume (our "higher-volume" trials) and a separatory funnel resulted in more reproducible results. The higher-volume trials had an additional benefit in that four subsamples could be collected from different elevations in the separatory funnel. This allowed for characterizing the distribution of oil within the sample and enabled the theoretical calculation of particle size based on terminal rise velocity.

By combining the results from effectiveness tests, interfacial tension measurements, and drop size measurements we have developed a conceptual model of oil-dendritic polymer interactions and a description of the possible mechanisms of oil dispersion. Dendritic polymers are characterized by what can be thought of as an amphiphilic structure with the hydrophilic end groups at the surface and less hydrophilic regions in the interior. When interacting with crude oil hydrocarbon molecules appear to penetrate the polymer surface and adsorb inside the polymer. Some large hydrocarbons could partially protrude into the polymer with tails that remain in the bulk oil droplet. These can be thought of as hydrocarbon bridges since they link the polymers to the oil drops (see Figure 6-1). Dendritic polymers may adsorb onto the oil droplet surface through these hydrocarbon bridges reducing the oil/water interfacial tension and coating the droplets with hydrophilic external surface groups that enable a more stable emulsion. Because the polymers behave like particles on the surface, this can be thought of as a Pickering emulsion mechanism. This may be possible even without the hydrocarbon bridges, but because the effectiveness data and previous work (Geitner et al. 2012) suggest hydrocarbon uptake into the

polymer and the formation of polymer/oil aggregates, the hydrocarbon bridge model seems likely.

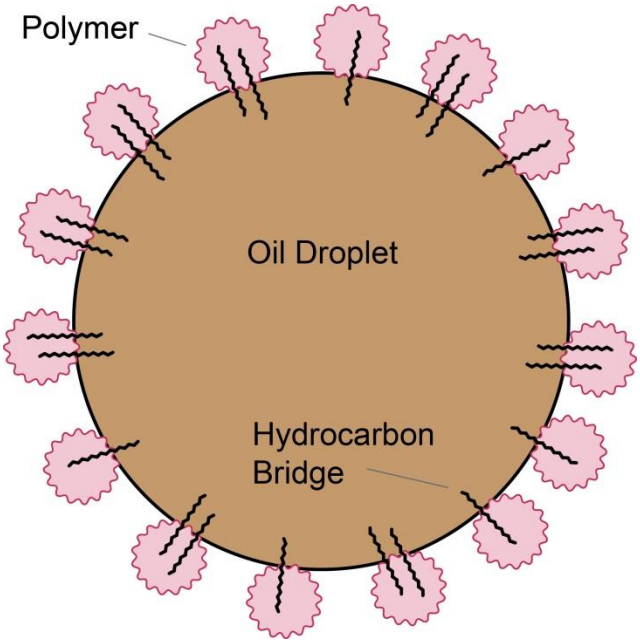

Figure 6-1 Conceptual model for dendritic polymer interaction with crude oil.

Small dendritic polymers with limited interior space were not effective, probably because they cannot hold hydrocarbons inside. Even though they were shown to decrease the interfacial tension at high concentrations, that effect was not sufficient to produce stable emulsions.

The charge of surface functional groups on the exterior of the dendritic polymers had a significant impact on the interactions between the oil and polymers. Crude oil drops typically display negative charges in water (Marinova *et al.* 1996). Polymers with positive surface charge would be attracted electrostatically to the oil drops and the polymers with negative charge would be repelled. Our data were consistent with this model, since the positively charged dendrimers were more effective than the neutral or negatively charged dendrimers. It is possible that electrostatic interactions alone were responsible for the polymers adhering to and stabilizing the oil emulsion, and that hydrocarbon uptake or bridging was less important.

6.2 Recommended future studies

Effectiveness tests in this study were based on mass ratios, which means that the polymers with larger molecular weight had fewer molecules in solution. This could be one of the reasons that the effectiveness of 70 kDa and 750 kDa HY-PEI were less than that of the 10 kDa material. Further experiments with equal molar ratios (or a range of molar concentrations) could help elucidate the mechanisms further by testing whether the per-polymer hydrocarbon uptake is consistent across concentrations; this would help us understand the importance of encapsulation as a dispersion mechanism.

The effectiveness of dendritic polymers with other surface functional groups should also be examined. Surface charge is an apparently important reason for different performance on oil dispersion; however, besides the electrostatic forces other interactions between surface groups and oil molecules, such as van der Waals forces may also influence the effectiveness. Polymers with equal charge but different functional group structures are recommended for further work. Ideally, negatively charged functional groups that are still effective at dispersion could be found. These should be less toxic than the positively charge polymers we mostly used in this study. pH and ionic strength are also important factors to be examined. pH will alter the surface charge of the polymer and ionic strength will influence the electrical double layer formation and electrostatic repulsion between the oil droplets.

Even after our size measurement attempts, the relationship between the drop size distribution and size of the polymer remains unclear. Previous studies showed that the smaller the droplet size, the more stable the system. The optimal size of the polymer and how the size influences the structure of the oil-polymer complex should be further examined. This is difficult, as noted in our work, because typical size measurement techniques often fail under the dynamic

conditions of crude oil in water emulsions; more robust methods should be developed or learned from others.

According to interfacial tension data, dendritic polymers share a similar mechanism with surfactants, which disperse oil by reducing the interfacial tension. However, unlike surfactants, dendritic polymers seem to lack a key characteristic: the CMC. Without being able to measure a CMC we cannot *a priori* determine the best polymer/oil ratio as is done with surfactants. Understanding which other physical parameters beside the CMC—parameters that can be easily measured for dendritic polymers—would be most predictive of dispersant effectiveness would be a significant step forward in this field.

REFERENCES

AFP (2010) BP Oil Well Gushed 4.9 Million Barrels: US.

Amir, R. J., Pessah, N., Shamis, M. & Shabat, D. (2003) Self-immolative dendrimers. *Angewandte Chemie International Edition* **42**: 4494–4499.

Arkas, M., Tsiourvas, D. & Paleos, C. M. (2003) Functional Dendrimeric "Nanosponges" for the Removal of Polycyclic Aromatic Hydrocarbons from Water. *Chemistry of Materials* **15**: 2844–2847.

Aveyard, R., Binks, B. P. B. & Clint, J. J. H. (2003) Emulsions stabilised solely by colloidal particles. *Advances in Colloid and Interface Science* **100-102**: 503–546.

Belore, R. & Ross, S. (2000) Laboratory study to compare the effectiveness of chemical dispersants when applied dilute versus neat. *Proceedings of the Arctic and Marine Oil spill Program Technical Seminar, Environment Canada*.

Bhattacharya, P., Geitner, N. K., Sarupria, S. & Ke, P. C. (2013) Exploiting the physicochemical properties of dendritic polymers for environmental and biological applications. *Physical chemistry chemical physics : PCCP* **15**: 4477–90.

Binks, B. P. (2002) Particles as surfactants—similarities and differences. *Current Opinion in Colloid & Interface Science* **7**: 21–41.

Binks, B. P. & Fletcher, P. D. I. (2001) Particles Adsorbed at the Oil−Water Interface: A Theoretical Comparison between Spheres of Uniform Wettability and "Janus" Particles. *Langmuir* **17**: 4708–4710.

Bowers, A. S., Reid, H. L., Greenidge, A., Landis, C. & Reid, M. (2013) Blood viscosity and the expression of inflammatory and adhesion markers in homozygous sickle cell disease subjects with chronic leg ulcers. *PloS One* **8**.

Brochu, C., Pelletier, E., Caron, G. & Desnoyers, J. E. (1986) Dispersion of crude oil in seawater: The role of synthetic surfactants. *Oil and Chemical Pollution* **3**: 257–279.

C&EN (2010) BP's Ever-Growing Oil Spill.

Cai, C. & Chen, Z. Y. (1998) Intrinsic Viscosity of Starburst Dendrimers. *Macromolecules* **31**: 6393–6396.

Cakara, D. & Borkovec, M. (2007) Microscopic protonation mechanism of branched polyamines: poly (amidoamine) versus poly (propyleneimine) dendrimers. *Croatica chemica acta* **80**: 421–428.

Chandrasekar, S., Sorial, G. & Weaver, J. (2006) Dispersant effectiveness on oil spills – impact of salinity. *ICES Journal of Marine Science* **63**: 1418–1430.

Chen, J.-D. (1985) A model of coalescence between two equal-sized spherical drops or bubbles. *Journal of Colloid and Interface Science* **107**: 209–220.

Chen, W., Porcar, L., Liu, Y., Butler, P. D. & Magid, L. J. (2007) Small Angle Neutron Scattering Studies of the Counterion Effects on the Molecular Conformation and Structure of Charged G4 PAMAM Dendrimers in Aqueous Solutions. *Macromolecules* **40**: 5887–5898.

Cheng, P. & Neumann, A. W. (1992) Computational evaluation of axisymmetric drop shape analysis-profile (ADSA-P). *Colloids and Surfaces* **62**: 297–305.

Ciolkowski, M., Rozanek, M., Bryszewska, M. & Klajnert, B. (2013) The influence of PAMAM dendrimers surface groups on their interaction with porcine pepsin. *Biochimica et biophysica acta* **1834**: 1982–7.

Clayton, J. R., Payne, J. R. & Farlow, J. S. (1993) *Oil Spill Dispersants: Mechanisms of Action and Laboratory Tests*. CRC Press.

Cooper, A., Londono, J., Wignall, G., McClain, J., Samulski, E., Lin, J., Dobrynin, A., Rubinstein, M., Burke, A., Frechet, J. & DeSimone, J. (1997) Extraction of a hydrophilic compound from water into liquid CO2 using dendritic surfactants. *Nature* **389**: 368–371.

Coulter, W. (1953) Means for counting particles suspended in a fluid. 1953. *US Patent*.

Deshiikan, S. & Papadopoulos, K. (1995) London-vdW and EDL effects in the coalescence of oil drops. *Journal of colloid and interface science*: 302–312.

Diallo, M. S., Balogh, L., Shafagati, A., Johnson,, J. H., Goddard, W. A. & Tomalia, D. A. (1999) Poly(amidoamine) Dendrimers: A New Class of High Capacity Chelating Agents for Cu(II) Ions. *Environmental Science & Technology* **33**: 820–824.

Diallo, M. S., Falconer, K. & Johnson,, J. H. (2007*a*) Dendritic Anion Hosts: Perchlorate Uptake by G5-NH 2 Poly(propyleneimine) Dendrimer in Water and Model Electrolyte Solutions. *Environmental Science & Technology* **41**: 6521–6527.

Diallo, M. S., Falconer, K., Johnson, J. H. & Goddard, W. A. (2007*b*) Dendritic anion hosts: perchlorate uptake by G5-NH2 poly(propyleneimine) dendrimer in water and model electrolyte solutions. *Environmental science & technology* **41**: 6521–6527.

Diallo, M. S., Arasho, W., Johnson, J. H. & Goddard, W. A. (2008) Dendritic chelating agents. 2. U(VI) binding to poly(amidoamine) and poly(propyleneimine) dendrimers in aqueous solutions. *Environmental science & technology* **42**: 1572–1579.

Etkin, D. S. (2001) ANALYSIS OF OIL SPILL TRENDS IN THE UNITED STATES AND WORLDWIDE. *International Oil Spill Conference Proceedings* **2001**: 1291–1300.

Farrington, P. & Hawker, C. (1998) The melt viscosity of dendritic poly (benzyl ether) macromolecules. *macromolecules* **31**: 5043–50.

Fingas, M. (2011) Oil Spill Dispersants: A Technical Summary. *Oil spill science and technology : prevention, response, and cleanup* pp. 435–582. Elsevier/Gulf Professional Pub.

Fingas, M. & Advisory, P. C. (2002) A review of literature related to oil spill dispersants especially relevant to Alaska. *Prince William Sound Regional citizens advisory Council (PWSRCAC) Anchorage, Alaska*.

Fingas, M. F., Dufort, V. M., Hughes, K. A., Bobra, M. A. & Duggan, L. V. (1989) *Oil Dispersants: New Ecological Approaches, Issue 1018*. ASTM International.

Fiocco, R. J. & Lewis, A. (1999) Oil Spill Dispersants. *Pure and Applied Chemistry* **71**: 27–42.

De Folter, J. W. J., van Ruijven, M. W. M. & Velikov, K. P. (2012) Oil-in-water Pickering emulsions stabilized by colloidal particles from the water-insoluble protein zein. *Soft Matter* **8**: 6807.

Geitner, N. K., Bhattacharya, P., Steele, M., Chen, R., Ladner, D. a. & Ke, P. C. (2012) Understanding dendritic polymer–hydrocarbon interactions for oil dispersion. *RSC Advances* **2**: 9371.

Girault, H. H. ., Schiffrin, D. . & Smith, B. D. . (1984) The measurement of interfacial tension of pendant drops using a video image profile digitizer. *Journal of Colloid and Interface Science* **101**: 257–266.

Glaser, N., Adams, D. J., Böker, A. & Krausch, G. (2006) Janus particles at liquid-liquid interfaces. *Langmuir : the ACS journal of surfaces and colloids* **22**: 5227–5229.

Gong, Y., Zhao, X., Cai, Z., O'Reilly, S. E., Hao, X. & Zhao, D. (2014) A review of oil, dispersed oil and sediment interactions in the aquatic environment: influence on the fate, transport and remediation of oil spills. *Marine pollution bulletin* **79**: 16–33.

Grinstaff, M. W. (2002) Biodendrimers: New Polymeric Biomaterials for Tissue Engineering. *Chemistry - A European Journal* **8**: 2838.

Hemmer, M. J., Barron, M. G., and Greene, R. M. (2010) Comparative Toxicity of Louisiana Sweet Crude Oil (LSC) and Chemically Dispersed LSC to Two Gulf of Mexico Aquatic Test Species. *US EPA/ORD National Health and Environmental Effects Research Laboratory*.

Honary, S., Ebrahimi, P. & Hadianamrei, R. (2014) Optimization of particle size and encapsulation efficiency of vancomycin nanoparticles by response surface methodology. *Pharmaceutical development and technology* **19**: 987–998.

Hult, A., Johansson, M. & Malmstrom, E. (1999) Hyperbranched polymers. *BRANCHED POLYMERS II* **143**: 1–34.

Inoue, K. (2000) Functional dendrimers, hyperbranched and star polymers. *Progress in Polymer Science* **25**.

Israelachvili, J. N. (2011) *Intermolecular and Surface Forces: Revised Third Edition*. Academic Press.

Israelachvili, J. N., Mitchell, D. J. & Ninham, B. W. (1976) Theory of self-assembly of hydrocarbon amphiphiles into micelles and bilayers. *Journal of the Chemical Society, Faraday Transactions 2* **72**: 1525.

Ivanov, I. B., Danov, K. D. & Kralchevsky, P. a. (1999) Flocculation and coalescence of micron-size emulsion droplets. *Colloids and Surfaces A: Physicochemical and Engineering Aspects* **152**: 161–182.

Jennings, J. W. & Pallas, N. R. (1988) An efficient method for the determination of interfacial tensions from drop profiles. *Langmuir* **4**: 959–967.

Kaku, V., Boufadel, M. & Venosa, A. (2006) Evaluation of mixing energy in laboratory flasks used for dispersant effectiveness testing. *Journal of Environment Engineering* **132**: 93–101.

Khan, A. & Shah, S. (2008) Determination of critical micelle concentration (cmc) of sodium dodecyl sulfate (SDS) and the effect of low concentration of pyrene on its cmc using ORIGIN software. *Journal of Chemical Society of Pakistan* **30**.

Khelifa, A., Fieldhouse, B., Wang, Z., Yang, C., Landriault, M., Brown, C. E. & Fingas, M. (2006) Effects of chemical dispersant on oil sedimentatiion due to oil-SPM flocculation: experiments with the nist standard reference material 1941B. *2008 International oil spill conference* pp. 627–632.

Kim, Y. (1998) Hyperbranched polymers 10 years after. *Journal of Polymer Science Part A Polymer Chemistry*: 1685–1698.

Kim, Y. & Webster, O. (1992) Hyperbranched polyphenylenes. *Macromolecules* **25**.

Kruss company (2012) Software for Drop Shape Analysis DSA1 User Manual.

Kulp, S., Yang, Y., Hung, C. & Chen, K. (2004) 3-phosphoinositide-dependent protein kinase-1/Akt signaling represents a major cyclooxygenase-2-independent target for celecoxib in prostate cancer cells. *Cancer research* **15**: 1444–1451.

Lee, C. C., MacKay, J. a, Fréchet, J. M. J. & Szoka, F. C. (2005) Designing dendrimers for biological applications. *Nature biotechnology* **23**: 1517–26.

Lessard, R. & DeMarco, G. (2000) The significance of oil spill dispersants. *Spill Science & Technology Bulletin* **6**.

Li, M. & Garrett, C. (1998) The relationship between oil droplet size and upper ocean turbulence. *Marine Pollution Bulletin* **36**: 961–970.

Lin, S.-T., Maiti, P. K. & Goddard, W. a (2005) Dynamics and thermodynamics of water in PAMAM dendrimers at subnanosecond time scales. *The journal of physical chemistry. B* **109**: 8663–72.

Macedo, A. S., Quelhas, S., Silva, A. M. & Souto, E. B. (2014) Nanoemulsions for delivery of flavonoids: formulation and in vitro release of rutin as model drug. *Pharmaceutical development and technology* **19**: 677–80.

Mackay, D. & Hossain, K. (1982) Interfacial tensions of oil, water, chemical dispersant systems. *The Canadian Journal of Chemical Engineering* **60**: 546–550.

Maiti, P. K. & Goddard, W. A. (2006) Solvent quality changes the structure of G8 PAMAM dendrimer, a disagreement with some experimental interpretations. *The journal of physical chemistry. B* **110**: 25628–32.

Magnet Lab, National High Magnetic Field Laboratory (2014) What's in an oil drop. http://www.magnet.fsu.edu/education/tutorials/magnetacademy/fticr/page4.html. Accessed July 2014.

Marinova, K., Alargova, R. & Denkov, N. (1996) Charging of oil-water interfaces due to spontaneous adsorption of hydroxyl ions. *Langmuir* **4**: 2045–2051.

Matthews, O., Shipway, A. & Stoddart, J. (1998) Dendrimers—branching out from curiosities into new technologies. *Progress in Polymer Science* **23**.

Meijer, E. W. & Van Genderen, M. H. P. (2003) Chemistry: dendrimers set to self-destruct. *Nature* **426**: 128–9.

Morais, D. (2006) Evaluation of the surface tension of poly (vinyl butyral) using the pendant drop method. *Macromolecular …* **245-246**: 208–214.

Mukherjee, B. & Wrenn, B. A. B. (2011) Effects of Physical Properties and Dispersion Conditions on the Chemical Dispersion of Crude Oil. *Environmental Engineering …* **28**: 263–273.

Murat, M. & Grest, G. S. (1996) Molecular Dynamics Study of Dendrimer Molecules in Solvents of Varying Quality. *Macromolecules* **29**: 1278–1285.

Nalco Environmental Solutions, LLC (2011) COREXIT® Ingredients. http://www.nalcoesllc.com/nes/1602.htm, Accessed July 2014.

NCR (2005) *Oil Spill Dispersants: Efficacy and Effects*. The National Academies Press.

Newkome, G. R., Young, J. K., Baker, G. R., Potter, R. L., Audoly, L., Cooper, D., Weis, C. D., Morris, K. & Johnson, C. S. (1993) Cascade polymers. 35. pH dependence of hydrodynamic radii of acid-terminated dendrimers. *Macromolecules* **26**: 2394–2396.

Nisato, G., Ivkov, R. & Amis, E. J. (2000) Size Invariance of Polyelectrolyte Dendrimers. *Macromolecules* **33**: 4172–4176.

Noor El-Din, M. R., El-Gamal, I. M., El-Hamouly, S. H., Mohamed, H. M., Mishrif, M. R. & Ragab, A. M. (2013) Rheological behavior of water-in-diesel fuel nanoemulsions stabilized by mixed surfactants. *Colloids and Surfaces A: Physicochemical and Engineering Aspects* **436**: 318–324.

NRC (2005) *Oil Spill Dispersants: Efficacy and Effects*. National Academies Press; 1 edition.

Patton, J. S., Rigler, M. W., Boehm, P. D. & Fiest, D. L. (1981) Ixtoc 1 oil spill: flaking of surface mousse in the Gulf of Mexico. *Nature* **290**: 235–238.

Pickering, S. U. (1907) CXCVI.Emulsions. *Journal of the Chemical Society, Transactions* **91**: 2001.

Piispanen, P. (2002) Synthesis and characterization of surfactants based on natural products. *Kungl Tekniska Högskolan, Stockholm*.

Reichert, M. & Walker, L. (2013) Interfacial Tension Dynamics, Interfacial Mechanics, and Response to Rapid Dilution of Bulk Surfactant of a Model Oil–Water-Dispersant System. *Langmuir* **29**: 1857–67.

Rewick, R. T., Sabo, K. A. & Smith, J. H. (1984) The Drop-Weight Interfacial Tension Method for Predicting Dispersant Performance. *Oil Spill Chemical Dispersants: Research, Experience, and Recommendations* pp. 94–107.

Reynolds, R. A., Stramski, D., Wright, V. M. & Woźniak, S. B. (2010) Measurements and characterization of particle size distributions in coastal waters. *Journal of Geophysical Research* **115**: C08024.

Saha, A. & Nikova, A. (2013) Oil Emulsification Using Surface-Tunable Carbon Black Particles. *Applied Materials & Sciences*: 3094–3100.

Schramm, L. L., Stasiuk, E. N. & Marangoni, D. G. (2003) Surfactants and their applications. *Annual Reports on the Progress of Chemistry* **99**: 3–48.

Seebach, D., Herrmann, G. F., Lengweiler, U. D., Bachmann, B. M. & Amrein, W. (1996) Synthesis and Enzymatic Degradation of Dendrimers from(R)-3-Hydroxybutanoic Acid and Trimesic Acid. *Angewandte Chemie International Edition in English* **35**: 2795–2797.

Seiler, M. (2002) Dendritic Polymers - Interdisciplinary Research and Emerging Applications from Unique Structural Properties. *Chemical Engineering & Technology* **25**: 237–253.

Shpigelman, A., Shoham, Y., Israeli-Lev, G. & Livney, Y. D. (2014) β-Lactoglobulin–naringenin complexes: Nano-vehicles for the delivery of a hydrophobic nutraceutical. *Food Hydrocolloids* **40**: 214–224.

Sjoblom, J. (2005) *Emulsions and Emulsion Stability: Surfactant Science Series*. Bergen, Norway: CRC Press.

Smet, M., Liao, L.-X., Dehaen, W. & McGrath, D. V. (2000) Photolabile Dendrimers Using o -Nitrobenzyl Ether Linkages. *Organic Letters* **2**: 511–513.

Sorial, G., Venosa, A. & Koran, K. (2004*a*) Oil spill dispersant effectiveness protocol. I: Impact of operational variables. *Journal of Environment Engineering* **130**: 1073–1085.

Sorial, G. A. G., Venosa, A. A. D., Koran, K. K. M., Holder, E. & King, D. W. (2004*b*) Oil spill dispersant effectiveness protocol. I: Impact of operational variables. *Journal of Environment Engineering* **130**: 1073–1085.

Speight, J. G. (2006) *The Chemistry and Technology of Petroleum, Fourth Edition*. CRC Press.

Stechemesser, S. & Eimer, W. (1997) Solvent-Dependent Swelling of Poly(amido amine) Starburst Dendrimers. *Macromolecules* **30**: 2204–2206.

Sterling, M. C., Bonner, J. S., Ernest, A. N. S., Page, C. a & Autenrieth, R. L. (2004) Chemical dispersant effectiveness testing: influence of droplet coalescence. *Marine pollution bulletin* **48**: 969–77.

Sunder, A., Hanselmann, R., Frey, H. & Mülhaupt, R. (1999) Controlled synthesis of hyperbranched polyglycerols by ring-opening multibranching polymerization. *Macromolecules*: 4240–4246.

Tadros, T. (2009) Emulsion science and technology: a general introduction. *Emulsion science and technology. Wiley-VCH, …*: 1–56.

Tadros, T. F. (2013) *Emulsion Formation and Stability*. Weinheim, Germany: Wiley-VCH Verlag GmbH & Co. KGaA.

Tadros, T. F. & Vincent, B. (1983) Emulsion stability. *Encyclopedia of Emulsion Technology* **1**: 129–285.

Tawfiq, N. & Olsen, D. A. (1993) Saudi Arabia's response to the 1991 Gulf oil spill. *Marine Pollution Bulletin* **27**: 333–345.

Tomalia, D., Baker, H., Dewald, J. & Hall, M. (1985) A new class of polymers: starburst-dendritic macromolecules. *Polymer Journal*.

Torchilin, V. P. (2001) Structure and design of polymeric surfactant-based drug delivery systems. *Journal of controlled release : official journal of the Controlled Release Society* **73**: 137–72.

Venkataraman, P. & Tang, J. (2013) Attachment of a Hydrophobically Modified Biopolymer at the Oil–Water Interface in the Treatment of Oil Spills. *Applied Materials and Interfaces*: 3572–3580.

Venosa, A., King, D. & Sorial, G. (2002) The baffled flask test for dispersant effectiveness: a round robin evaluation of reproducibility and repeatability. *Spill Science & Technology Bulletin* **7**: 299–308.

Wahl-Jensen, V., Chapman, J., Asher, L., Fisher, R., Zimmerman, M., Larsen, T. & Hooper, J. W. (2007) Temporal analysis of Andes virus and Sin Nombre virus infections of Syrian hamsters. *Journal of virology* **81**: 7449–62.

Walstra, P. & Oortwijn, H. (1969) Estimating globule-size distribution of oil-in-water emulsions by coulter counter. *Journal of Colloid and Interface Science* **29**: 424–431.

Watanabe, S., Sato, M., Sakamoto, S., Yamaguchi, K. & Iwamura, M. (2000) New Dendritic Caged Compounds: Synthesis, Mass Spectrometric Characterization, and Photochemical Properties of Dendrimers with α-Carboxy-2-nitrobenzyl Caged Compounds at Their Periphery. *Journal of the American Chemical Society* **122**: 12588–12589.

Woodward, R. (1948) Surface tension measurements using the drop shape method. *Technical Guide*.

Ye, A., Zhu, X. & Singh, H. (2013) Oil-in-water emulsion system stabilized by protein-coated nanoemulsion droplets. *Langmuir : the ACS journal of surfaces and colloids* **29**: 14403–10.

Young, J. K., Baker, G. R., Newkome, G. R., Morris, K. F. & Johnson, C. S. (1994) "Smart" Cascade Polymers. Modular Syntheses of Four-Directional Dendritic Macromolecules with Acidic, Neutral, or Basic Terminal Groups and the Effect of pH Changes on Their Hydrodynamic Radii. *Macromolecules* **27**: 3464–3471.

Zeng, F. & Zimmerman, S. C. (1997) Dendrimers in Supramolecular Chemistry: From Molecular Recognition to Self-Assembly. *Chemical reviews* **97**: 1681–1712.

Zhang, H., Chon, C. H., Pan, X. & Li, D. (2009) Methods for counting particles in microfluidic applications. *Microfluidics and Nanofluidics* **7**: 739–749.

Zhang, W., Tichy, S. E., Pérez, L. M., Maria, G. C., Lindahl, P. A. & Simanek, E. E. (2003) Evaluation of multivalent dendrimers based on melamine: kinetics of thiol-disulfide exchange depends on the structure of the dendrimer. *Journal of the American Chemical Society* **125**: 5086–94.